

Individual based SIS models on (not so) dense large random networks

Jean-François Delmas ^{*} Paolo Frasca [†] Federica Garin [‡] Viet Chi Tran [§]
Aurélien Velleret [¶] Pierre-André Zitt ^{||}

September 10, 2024

Abstract

Starting from a stochastic individual-based description of an SIS epidemic spreading on a random network, we study the dynamics when the size n of the network tends to infinity. We recover in the limit an infinite-dimensional integro-differential equation studied by Delmas, Dronnier and Zitt (2022) for an SIS epidemic propagating on a graphon. Our work covers the case of dense and sparse graphs, provided that the number of edges grows faster than n , but not the case of very sparse graphs with $O(n)$ edges. In order to establish our limit theorem, we have to deal with both the convergence of the random graphs to the graphon and the convergence of the stochastic process spreading on top of these random structures: in particular, we propose a coupling between the process of interest and an epidemic that spreads on the complete graph but with a modified infection rate.

MSC2000: 05C80, 92D30, 60F99.

Keywords: Random graph, mathematical models of epidemics, measure-valued process, large network limit, limit theorem, graphon.

Acknowledgments: This work was financed by the Labex Bézout (ANR-10-LABX-58) and the COCOON grant (ANR-22-CE48-0011), and by the platform MODCOV19 of the National Institute of Mathematical Sciences and their Interactions of CNRS. V.C.T. is partly financed by the Chaire “Modélisation Mathématique et Biodiversité” of Veolia-Ecole Polytechnique-Museum National d’Histoire Naturelle-Fondation X. The research leading to this article was largely performed while A. Velleret was a researcher at LAMA and at GIPSA-Lab.

Accepted at ALEA: <https://doi.org/10.30757/ALEA.v21-52>

1 Introduction

We consider the spread of diseases with potential reinfections in large heterogeneous populations structured by random networks. We focus on SIS models, in which the population is partitioned

^{*}Cermics, Ecole des Ponts, France; E-mail: jean-francois.delmas@enpc.fr

[†]Univ. Grenoble Alpes, CNRS, Inria, Grenoble INP, GIPSA-Lab, 38000 Grenoble, France; E-mail: paolo.frasca@gipsa-lab.fr

[‡]Univ. Grenoble Alpes, Inria, CNRS, Grenoble INP, GIPSA-Lab, 38000 Grenoble, France; E-mail: federica.garin@inria.fr

[§]LAMA, Univ Gustave Eiffel, Univ Paris Est Creteil, CNRS, F-77454 Marne-la-Vallée, France; IRL 3457, CRM-CNRS, Université de Montréal, Canada; E-mail: chi.tran@univ-eiffel.fr

[¶]Université Paris-Saclay, INRAE, MaIAGE, F-78350 Jouy-en-Josas, France; E-mail: velleret@phare.normalesup.org, corresponding author

^{||}LAMA, Univ Gustave Eiffel, Univ Paris Est Creteil, CNRS, F-77454 Marne-la-Vallée, France; E-mail: Pierre-Andre.Zitt@univ-eiffel.fr

into two classes, namely S for susceptible individuals and I for infected ones. Infected individuals can transmit the disease to susceptible ones if they are in contact through the social network. Infected individuals remain infectious until their recovery, which is assumed to be spontaneous. The susceptibility and infectivity of individuals as well as their degrees in the social network can be heterogeneous, which makes the dynamics of such systems very complex. In this paper, we are interested in establishing limit theorems showing that, in large population, the possibly complex dynamics of the epidemics can be approximated by a system of integro-differential equations.

To be more precise, we start from a stochastic individual-based model of a finite population of size n , where each individual i in the population is characterized by a feature x_i that belongs to a generic space \mathbb{X} (assumed to be metric, separable and complete). One may think of the feature being a group label (so that \mathbb{X} can be discrete), or the individual's age (so that $\mathbb{X} = \mathbb{R}_+$), or their location (so that \mathbb{X} can be the sphere or \mathbb{R}^d), or a combination of those. The distribution of features in the population can be encoded by the (possibly random) measure:

$$\mu^{(n)}(dx) = \frac{1}{n} \sum_{i=1}^n \delta_{x_i}(dx).$$

The social contacts in the population are modeled by a random network, $G^{(n)}$, which is fixed in time: a contact between individuals i and j means that the edge (i, j) belongs to $G^{(n)}$, which happens with probability $w_E^{(n)}(x_i, x_j)$ depending on their respective features independently of all other edges. Each individual i is, at time t , in a state, say E_t^i , which is either S (susceptible) or I (infected). The initial condition is completely characterized by the (possibly random) sequences $\mathcal{X}^{(n)} = (x_i)_{i \in [1, n]}$ and $\mathcal{E}^{(n)} = (E_0^i)_{i \in [1, n]}$. At time t , if i is infected, that is $E_t^i = I$, then it recovers at rate $\gamma^{(n)}(x_i) \geq 0$, also depending on its feature; if i is susceptible, that is $E_t^i = S$, then it can be infected by individual j at rate $w_I^{(n)}(x_i, x_j)$ provided that i and j are connected (in $G^{(n)}$) and j is infected. At time t , we describe the infected population with the measure $\eta_t^{I, (n)}$ on \mathbb{X} given by:

$$\eta_t^{I, (n)}(dx) = \frac{1}{n} \sum_{i=1}^n \mathbb{1}_{\{E_t^i = I\}} \delta_{x_i}(dx). \quad (1.1)$$

Our main result, see Theorem 2.7 for a precise statement, is on the convergence of the processes $\eta^{I, (n)} = (\eta_t^{I, (n)})_{t \in \mathbb{R}_+}$ to a deterministic process $\eta^I = (\eta_t^I)_{t \in \mathbb{R}_+}$ of the form:

$$\eta_t^I(dx) = u(t, x) \mu(dx), \quad (1.2)$$

where the probability measure $\mu(dx)$, namely the limit of the sequence $\mu^{(n)}$, represents the probability for an individual of the population taken at random to have feature x , and $u(t, x)$ represents the probability for an individual with feature x to be infected at time t . We will show that the function $(u(t, x), t \in \mathbb{R}_+, x \in \mathbb{X})$ is the unique solution of the integro-differential equation:

$$\partial_t u(t, x) = (1 - u(t, x)) \int_{\mathbb{X}} u(t, y) w(x, y) \mu(dy) - \gamma(x) u(t, x), \quad (1.3)$$

with initial condition $u(0, \cdot) = u_0$, where $u_0(x)$ is the probability for an individual with feature x to be infected at time 0. In (1.3), the function $w(x, y)$ will be interpreted as a transmission kernel from (infected) individuals with feature y to (susceptible) individuals with feature x , and contains information on both the network and the transmission rate. The function $\gamma(x)$ can be interpreted as the recovery rate of (infected) individual with feature x , as $\gamma^{(n)}$ in the finite population model. For this convergence to hold, we assume, see Assumptions 2.3 and 2.6:

- a) **Convergence of the initial condition.** The distribution of the features $\mu^{(n)}$ in the population converges to a limit measure μ (for the weak topology on non-negative measures). The

initial distribution of the infected population $\eta_0^{I,(n)}$ converges to a deterministic limit η_0^I , with $\eta_0^I(dx) = u_0(x) \mu(dx)$.

- b) **Uniform convergence and regularity of the limit parameters.** The recovery rate $\gamma^{(n)}$ as well as the average transmission rate $w^{(n)}$, given by the following formula for any $(x, y) \in \mathbb{X}^2$:

$$w^{(n)}(x, y) = n w_E^{(n)}(x, y) w_I^{(n)}(x, y),$$

converge uniformly to γ and w , which are respectively μ -a.e. and $\mu^{\otimes 2}$ -a.e. continuous. The scaling factor n appears naturally as $n w_E^{(n)}(x, y)$ corresponds to the density of contacts between an individual with feature x and the population with feature y (scaled by the measure $\mu(dy)$), where each of these contacts corresponds to a potential infection rate of $w_I^{(n)}(x, y)$.

- c) **Control on the infection rate.** We assume the following convergence in mean (see Assumption 2.6 for a precise and slightly more general statement):

$$\lim_{n \rightarrow \infty} \frac{1}{n^2} \sum_{i, j \in \llbracket 1, n \rrbracket} w_I^{(n)}(x_i, x_j) = 0, \quad (1.4)$$

meaning that the infection rate per edge is small on average over the population.

Our results cover in particular the case of dense and sparse graphs, when the total number of edges is scaled to be of order n^a with $a = 2$ and $a \in (1, 2)$ respectively (see Remark 2.5 below); this corresponds for example to $w_E^{(n)} \equiv n^{a-2}$ and thus $w_I^{(n)}$ of order n^{1-a} , by Assumption b) above. Notice that (1.4) trivially holds in this case. However, our method fails to cover very sparse graphs corresponding to $a = 1$ for which the number of edges is of order n thus $w_I^{(n)}$ of order 1, as (1.4) does not hold. Simulations, see Section 4.3, hint that, although a deterministic limit may be derived, this limit is nonetheless not suitably represented by the deterministic process (1.2)-(1.3). Yet, the very-sparse case triggered a large literature; in this direction, see the reference in the related works section below.

In the dense heterogeneous case ($a = 2$), if $w_E^{(n)}$ does not depend on n , and thus is equal to \bar{w}_E , and if $w_I^{(n)} = n^{-1} \bar{w}_I$, for some fixed kernels \bar{w}_E and \bar{w}_I , then we have $w = \bar{w}_E \bar{w}_I$. In this case the sequence of graphs, $G^{(n)}$, which models the connection in the population of size n , converges towards a graphon with parameter \bar{w}_E , see [Lov12, Part 3]. The quantity $\bar{w}_E(x, y)$ is understood as the density of connections between the population with feature x and the population with feature y . Then the kernel w can be seen as the result of weighting the graphon \bar{w}_E by another kernel \bar{w}_I , which represents the interaction rates between features. See Remark 2.4 below for further comment in this direction.

Related work. There has been a growing literature on epidemics spreading on graphs, and the interested reader can refer to [And98, AB00, PB19, Hou12, KMS17, New02, New03]. Scaling limits for such processes have been considered mostly when the characteristics of the graph are fixed: for instance, diseases spreading on fixed lattices or configuration model graphs with fixed degree distributions. Many points of view have been taken: with moment closures [Dur07, GKS20], or using limit theorems for semi-martingale processes [BN08, Vol08, Mil11, DDMT12, JLW14] or for branching processes [BR13]. In this literature, the graphs are *very sparse* with a degree distribution that does not depend on the size n of the population.

In the meantime, there has been also a growing interest in scaling limits for random graphs [BCL⁺11, Lov12]. In the present paper, we model the social network by a graph and obtain for the dense graph case (for $a = 2$ above), as limit when n tends to infinity, a dynamical system propagating

on a graphon. Limit theorems for dynamical systems on graphs converging to graphons have been considered in [BLRT22, KHT22, KT19]. In [KT19, BLRT22], this is done for systems of ordinary differential equations on the graph (or when the randomness of the individual-based model has been averaged first, and the graph limit is considered in a second time). In [KHT22], starting from the stochastic individual-based dynamics on a random graph as in the present work, it is proved that after a proper rescaling so that the graph converges to a graphon, the evolution of the susceptible and infected populations converge to the integro-differential equation (1.3), first introduced and studied in [DDZ22]-[DDZ23]. We improve the results from [KHT22] by taking into account propagation rates depending on the features, considering weaker assumptions on the parameters γ and w of the model, and most importantly identifying the global condition (1.4) on the mean infection rate as sufficient to get this convergence, generalizing in particular the possible range of the scaling parameters. We refer to Remark 2.10 for further comments.

Eventually, our assumptions on the regularity of w allow for a large variety of random graphs and of feature dependencies that include, for instance, geometric random graphs [Pen03] or stochastic block models [Abb18], see Remark 2.1 below.

We also cite [AN22, NP22, VFG20] for deterministic epidemic dynamics on graphons, and [ARGL22] for a finite agent model on the graphon. See also [vdHJvL10] for epidemic propagation on an Erdős-Rényi random graph in the critical window.

Scaling limits of the SIS epidemic process for a large number of individuals with homogeneous interactions are well-described, including the study of the dynamical system derived from the law of large numbers, the deviations prescribed by the central limit theorem or by the large deviation theory (see e.g. [AB00, Chapter 8.2] or [PB19, Part I]). Taking into account features with finite possible values is a direct extension. To tackle a more general feature dependency, we follow similar lines as in [FM04], where a mean-field kernel is introduced to represent local effects of competition between plants.

Outline. In Section 2, we present the stochastic individual-based model of SIS epidemic spreading on a random network. Two objects, both of random nature, are at the core of the study: a random graph $G^{(n)}$ of size $n \in \mathbb{N}$ and a sequence of stochastic measure-valued processes $(\eta^{(n)})_{n \in \mathbb{N}}$. We discuss the sparsity of the random graph and state our main convergence result in Theorem 2.7. The proof of the theorem, which is carried out in Section 3, follows a classical tightness-uniqueness scheme. First, tightness is proved in Section 3.2, which implies that the sequence $(\eta^{(n)})_{n \in \mathbb{N}}$ is relatively compact. Next, in Section 3.3, we show that the limiting values are solutions of a deterministic integro-differential equation: proving this fact requires a careful coupling argument that is developed in Appendix A. Finally, the uniqueness of the solution to the limiting equation, which is established in Section 3.4, allows us to conclude. A detailed discussion on the scope of our results and numerical simulations, with an emphasis on the limit behavior for very sparse graphs, are presented in Section 4.

2 Definition of the model and of the limiting equation

In this section we formally define the relevant mathematical objects and state our main result. After defining some useful notation in Section 2.1, we define the stochastic individual-based model in Section 2.2 and finally in Section 2.3 we define the limit graphon-based integro-differential equation and we state the main convergence result.

2.1 Notation

We denote by \mathbb{N}^* the set of positive integers and $\mathbb{N} = \mathbb{N}^* \cup \{0\}$. We also set $\llbracket 1, n \rrbracket = \{k \in \mathbb{N} : 1 \leq$

$k \leq n\}$ for $n \in \mathbb{N}^*$. For $a, b \in \mathbb{R}$, we write $a \wedge b$ for the minimum between a and b and $a \vee b$ for the maximum between a and b .

For a real-valued function defined on a set Ω , its supremum norm is:

$$\|f\|_\infty = \sup_{\Omega} |f|.$$

For a measurable space (Ω, \mathcal{F}) , we denote by $\mathcal{M}_1(\Omega)$ the set of probability measures on Ω . For $\mu \in \mathcal{M}_1(\Omega)$ and a real-valued measurable function f defined on Ω , we will sometimes denote the integral of f with respect to the measure μ , if well-defined, by $\langle \mu | f \rangle = \int_{\Omega} f(x) \mu(dx) = \int f d\mu$. For a bounded measurable real function F defined on \mathbb{R} and a bounded real-valued measurable function f on Ω , we define the real-valued measurable function F_f defined for $\mu \in \mathcal{M}_1(\Omega)$ by:

$$F_f(\mu) = F(\langle \mu | f \rangle). \quad (2.1)$$

For a metric space Ω endowed with its Borel σ -field, we endow $\mathcal{M}_1(\Omega)$ with the topology of weak convergence. We also denote by $\mathcal{D}(\mathbb{R}_+, \Omega)$ the space of right-continuous left-limited (càd-làg) paths from \mathbb{R}_+ to Ω . This space is endowed with the Skorokhod topology (see *e.g.* [Bil99, Chapter 3]).

In what follows (\mathbb{X}, d) will denote a Polish metric space (complete and separable). We shall write $\mathcal{M}_1 = \mathcal{M}_1(\mathbb{X} \times \{S, I\})$ (where \mathbb{X} is endowed with its Borel σ -field) and $\mathcal{D} = \mathcal{D}(\mathbb{R}_+, \mathcal{M}_1)$.

2.2 Individual-based model

We consider a population of $n \in \mathbb{N}^*$ individuals indexed by $i \in \llbracket 1, n \rrbracket$ and each characterized by a value $x_i^{(n)} \in \mathbb{X}$ (also called feature in what follows) and by an epidemiological state $E_t^{(n),i} \in \{S, I\}$, that varies over (continuous) time $t \in \mathbb{R}_+$ according to whether the individual i is susceptible or infected. We also set $\mathcal{X}^{(n)} = (x_i^{(n)})_{i \in \llbracket 1, n \rrbracket} \in \mathbb{X}^n$. To simplify notation, we shall write x_i and E_t^i for $x_i^{(n)}$ and $E_t^{(n),i}$. For a time $t \in \mathbb{R}_+$, the population is represented by the empirical probability measure $\eta_t^{(n)}$ on $\mathbb{X} \times \{S, I\}$ defined by:

$$\eta_t^{(n)}(dx, de) = \frac{1}{n} \sum_{i=1}^n \delta_{(x_i, E_t^i)}(dx, de). \quad (2.2)$$

This defines a process $(\eta_t^{(n)})_{t \in \mathbb{R}_+}$ taking values in the set \mathcal{M}_1 of probability measures on $\mathbb{X} \times \{S, I\}$ with initial condition:

$$\eta_0^{(n)}(dx, de) = \frac{1}{n} \sum_{i=1}^n \delta_{(x_i, E_0^i)}(dx, de). \quad (2.3)$$

Note that the measure $\eta_t^{I, (n)}$ defined in the introduction by Equation 1.1 corresponds to the restriction of the measure $\eta_t^{(n)}$ to the subset $\mathbb{X} \times \{I\}$. Since the individual features are kept fixed in time, the restriction $\eta_t^{S, (n)}$ of the measure $\eta_t^{(n)}$ to the complementary subset $\mathbb{X} \times \{S\}$ is actually deduced as in the following equation:

$$\eta_t^{S, (n)}(dx) = \frac{1}{n} \sum_{i=1}^n \mathbb{1}_{\{E_t^i=S\}} \delta_{x_i}(dx) = \mu^{(n)}(dx) - \eta_t^{I, (n)}(dx), \quad (2.4)$$

where $\mu^{(n)}(dx)$ is the marginal probability distribution in $x \in \mathbb{X}$ of $\eta_0^{(n)}(dx, de)$ (and thus of $\eta_t^{(n)}$ for all $t \in \mathbb{R}_+$):

$$\mu^{(n)}(dx) = \eta_0^{(n)}(dx, \{S, I\}) = \frac{1}{n} \sum_{i=1}^n \delta_{x_i}(dx). \quad (2.5)$$

Let us underline that the process $\eta^{(n)}$ is more suited than $\eta^{I \cdot (n)}$ to describe the convergence because the empirical distribution $\mu^{(n)}$ needs not be introduced as an additional parameter (in addition to the initial condition), see for example Proposition 2.2.

The heterogeneity between individual contacts is modelled by an undirected random graph $G^{(n)} = (V^{(n)}, E^{(n)})$ along which the disease is transmitted. The vertices $V^{(n)} = \llbracket 1, n \rrbracket$ represent the individuals and we assume that there is an edge between i and j , that is $(i, j) \in E^{(n)}$, with probability $w_E^{(n)}(x_i, x_j) \in [0, 1]$, and independently for any choice of $1 \leq i < j \leq n$. The function $w_E^{(n)}$ will be called the *connection density*. For an undirected graph, the measurable function $w_E^{(n)}$ is necessarily symmetric, *i.e.*, $w_E^{(n)}(x, y) = w_E^{(n)}(y, x)$ for all $x, y \in \mathbb{X}$. When (i, j) is an edge of $G^{(n)}$, we will write classically $i \sim_{G^{(n)}} j$ or $i \sim j$ when there is no ambiguity.

Remark 2.1 (Examples of random graphs). As said in the introduction, the Polish metric space of features (\mathbb{X}, d) parametrizes the latent variable assumed to explain the connections in the social network. In view of the graphons which will be considered, a classical choice is $\mathbb{X} = [0, 1]$ with independent uniform random features $\mathcal{X}^{(n)} = (x_i)$ (the reference measure μ is then the Lebesgue measure). However other choices are possible as well to cover several graph families.

- (i) **Complete graph.** For any choice of \mathbb{X} and individual features $\mathcal{X}^{(n)}$, choosing $w_E^{(n)} \equiv 1$ (that is, $w_E^{(n)}$ constant equal to 1) provides the complete graph where every pair of vertices is connected. The features $\mathcal{X}^{(n)}$ then simply affect the infection rate in a mean-field setting.
- (ii) **Geometric random graphs.** Choosing $\mathbb{X} = [0, 1]^d$, the $(x_i)_{i \leq n}$ independently and uniformly distributed over \mathcal{X} (according to the Lebesgue measure which is exactly μ) and $w_E^{(n)}(x, y) = \mathbb{1}_{\{|x-y| < r\}}$, for a constant $r > 0$, provides an example of geometric random graphs, see e.g. [Pen03]. A direct generalization corresponds to $w_E^{(n)}(x, y) = g(|x - y|)$ with a measurable $[0, 1]$ -valued function g .
- (iii) **Stochastic block models (SBM).** The SBM with $k \in \mathbb{N}^*$ classes corresponds to a population divided in k classes and can be represented using a finite state space $\mathbb{X} = \llbracket 1, k \rrbracket$. Up to reordering, $\mathcal{X}^{(n)}$ is then simply described by the proportion of individuals in each of the k classes, proportions that are assumed to converge to a certain discrete probability measure $\mu = (\mu^{(i)})_{i \in \llbracket 1, k \rrbracket}$. The symmetric function $w_E^{(n)}$ then takes a finite number of values. See e.g. [Abb18]. The SBM is a very common model for heterogeneous population. The particular case $k = 1$, where w_E is simply a constant, yields the Erdős-Rényi random graph, see e.g. [Bol79, vdH17].

In what follows, it is possible to consider $G^{(n)}$ a directed graph, with a slight modification of the arguments. However, for the sake of clarity and since undirected graphs are realistic for social interactions, in this paper we will focus on the case where $G^{(n)}$ is undirected, and in particular $w_E^{(n)}(x, y)$ is symmetric for all n .

We now describe the dynamics of the epidemics along the graph using propagation and recovery:

- (i) **Propagation.** Conditionally on i and j being connected and on i being susceptible and j infected, the disease can be transmitted along the edge at rate $w_I^{(n)}(x_i, x_j) \geq 0$. Each edge transmits the infection independently, so for a given susceptible individual i , the rate at which it becomes infected is:

$$\sum_{j \sim i} w_I^{(n)}(x_i, x_j) \mathbb{1}_{\{E_i^j = I\}}.$$

When the infection occurs, say at time t , the state of the population changes from $\eta_{t-}^{(n)}$ to:

$$\eta_t^{(n)} = \eta_{t-}^{(n)} - \frac{1}{n} \delta_{(x_i, S)} + \frac{1}{n} \delta_{(x_i, I)}.$$

- (ii) **Recovery.** An infected individual i recovers at rate $\gamma(x_i) > 0$. When the recovery occurs, say at time t , the state of the population changes from $\eta_{t-}^{(n)}$ to:

$$\eta_t^{(n)} = \eta_{t-}^{(n)} - \frac{1}{n} \delta_{(x_i, I)} + \frac{1}{n} \delta_{(x_i, S)}.$$

In all the paper, we will assume that the *recovery rate* $\gamma^{(n)}$, *infection rate* $w_I^{(n)}$, and *connection density* $w_E^{(n)}$ are measurable functions (respectively from \mathbb{X} to \mathbb{R}_+ , \mathbb{X}^2 to \mathbb{R}_+ and \mathbb{X}^2 to $[0, 1]$). Note that they depend only on the features of the individuals but not on time nor on times of infection events. These functions are kept constant throughout the epidemic, but the global infection and recovery rates, at the scale of the population, vary because the partition into susceptible and infected individuals changes with time.

The above ingredients define a pure-jump Markov dynamics, see Section 3.1. For the process $\eta^{(n)} = (\eta_t^{(n)})_{t \in \mathbb{R}_+}$ to be itself Markov, one needs an identifiability property, that is, to be able to recover the state of the individuals at time t from the measure $\eta_t^{(n)}$. Let us stress that we shall not use that the process $\eta^{(n)}$ is Markov nor the identifiability property to prove our main result, see Theorem 2.7. Nevertheless, we believe that the Markov property of $\eta^{(n)}$ deserves to be stated.

We say the model is *identifiable* if the elements of the sequence $(x_i)_{i \in \llbracket 1, n \rrbracket}$ (with x_i depending also on n) are pairwise distinct, or equivalently that the measure $\mu^{(n)}$ has exactly n atoms, all of them with mass $1/n$. When the model is not identifiable, there is always a natural way to obtain an identifiable model by enriching the space \mathbb{X} into $\mathbb{X}' = \mathbb{X} \times [0, 1]$: the feature of the individual i can be described for example by either $(x_i, i/n)$ or (x_i, U_i) , where $(U_i)_{i \in \mathbb{N}^*}$ are independent uniform random variables and independent of the initial condition.

Recall that $\mathcal{D} = \mathcal{D}(\mathbb{R}_+, \mathcal{M}_1)$ denotes the space of càd-làg functions taking values in $\mathcal{M}_1 = \mathcal{M}_1(\mathbb{X} \times \{S, I\})$ endowed with the Skorokhod topology. Recall also the notation $F_f(\eta) = F(\langle \eta | f \rangle)$ from (2.1).

Proposition 2.2 (Markov property of the process $\eta^{(n)}$). *Let $n \geq 1$ be fixed and assume the model is identifiable. Conditionally on the sequence $(x_i)_{i \in \llbracket 1, n \rrbracket}$ and on $G^{(n)}$, the process $\eta^{(n)} = (\eta_t^{(n)})_{t \in \mathbb{R}_+}$ is a Markov pure-jump process on \mathcal{M}_1 , and thus is \mathcal{D} -valued. Its generator $\mathcal{A}^{(n)}$ is characterized by the following expression, which applies to any bounded real-valued measurable function F defined on \mathbb{R} , to any bounded real-valued measurable function f on $\mathbb{X} \times \{S, I\}$ and to any point measure η with marginal probability distribution given by (2.5):*

$$\begin{aligned} \mathcal{A}^{(n)}(F_f)(\eta) &= \sum_{i=1}^n \mathbb{1}_{\{E^i=I\}} \gamma^{(n)}(x_i) \left(F_f\left(\eta - \frac{1}{n} \delta_{(x_i, I)} + \frac{1}{n} \delta_{(x_i, S)}\right) - F_f(\eta) \right) \\ &\quad + \sum_{i=1}^n \mathbb{1}_{\{E^i=S\}} \sum_{j \sim i} w_I^{(n)}(x_i, x_j) \mathbb{1}_{\{E^j=I\}} \left(F_f\left(\eta - \frac{1}{n} \delta_{(x_i, S)} + \frac{1}{n} \delta_{(x_i, I)}\right) - F_f(\eta) \right), \end{aligned} \quad (2.6)$$

where x_i and E^i denote the feature and epidemiological states of the i -th atom of η .

Proof. The process $\eta^{(n)}$ is of course constant between jump events given by infection or recovery events. The proof is then an immediate consequence of the description of the epidemic dynamics (see also the semi-martingale representation (3.5) below). Notice that in (2.6) the summation $\sum_{j \sim i}$ between neighboring pairs (i, j) can indeed be seen as a functional of the probability measure η with marginal probability distribution given by (2.5) thanks to the identifiability assumption. (The two other summations $\sum_{i=1}^n$ are functionals of the probability measure η without the identifiability assumption.)

Notice there is no accumulation of jump times for the process $\eta^{(n)}$ (conditionally on $\mathcal{X}^{(n)}$) as the jump rates $\gamma^{(n)}$ and $w_I^{(n)}$ are bounded on $\bar{\mathcal{X}}^{(n)} = \{x_i : i \in \llbracket 1, n \rrbracket\}$ and $(\bar{\mathcal{X}}^{(n)})^2$, since the state space for the process $\eta^{(n)}$ is in fact reduced to the probability measures on the finite set $\bar{\mathcal{X}}^{(n)} \times \{S, I\}$. \square

2.3 Convergence towards an epidemic spreading on a graphon

We consider now the case of a large graph, *i.e.* when n is large and tends to infinity. The network structure as well as the dynamics of the epidemic are suitably rescaled. We measure the overall propagation rate of the epidemic through the function $w^{(n)}$ defined on \mathbb{X}^2 by:

$$w^{(n)}(x, y) = n w_E^{(n)}(x, y) w_I^{(n)}(x, y), \quad (2.7)$$

as described in the introduction. The function $w^{(n)}$ captures the effect on the number of contacts (through $n w_E^{(n)}$) weighted by the intensity of interactions (that is, $w_I^{(n)}$).

Let $\eta_0 \in \mathcal{M}_1$ be a deterministic probability measure on $\mathbb{X} \times \{S, I\}$ with marginal μ on \mathbb{X} :

$$\eta_0(dx, de) = \mu(dx) \left((1 - u_0(x)) \delta_S(de) + u_0(x) \delta_I(de) \right), \quad (2.8)$$

where $\mu \in \mathcal{M}_1(\mathbb{X})$ and u_0 is a $[0, 1]$ -valued measurable function defined on \mathbb{X} . It is elementary to generalize the results when u_0 is also random, but we prefer to keep the result simple. The probability measure μ on \mathbb{X} will capture the asymptotic feature distribution of the individuals in the population and will be seen as the limit of $\mu^{(n)}$ introduced in (2.5). Let us set $\mu^{\otimes 2}(dx, dy) = \mu(dx)\mu(dy)$.

Assumption 2.3 (Structural conditions). We assume that:

- (i) For $n \in \mathbb{N}^*$, the process $(\eta_t^{(n)})_{t \in \mathbb{R}_+}$ is started from the initial condition $\eta_0^{(n)}$ of the form (2.3).
- (ii) The sequence $(\eta_0^{(n)})_{n \in \mathbb{N}^*}$ converges in probability to η_0 (in \mathcal{M}_1 endowed with the topology of the weak convergence).
- (iii) The sequence $(w^{(n)})_{n \in \mathbb{N}^*}$ converges uniformly to a (non-negative) transmission density kernel w which is bounded and $\mu^{\otimes 2}$ -a.e. continuous.
- (iv) The sequence $(\gamma^{(n)})_{n \in \mathbb{N}^*}$ converges uniformly to a (non-negative) recovery function γ which is bounded and μ -a.e. continuous.

Remark 2.4 (Transmission kernel $w(x, y) = \beta(x)w_E(x, y)\theta(y)$). In [DDZ22, Example 1.3], the authors propose to represent the transmission density kernel $w(x, y)$ from Assumption 2.3-(iii), as $\beta(x)w_E(x, y)\theta(y)$, where $\beta(x)$ captures the susceptibility of individuals with feature x , $\theta(y)$ the infectiousness of individuals with feature y , while $w_E(x, y)$ relates to the contact rate between individuals with features respectively x and y . For example, using (2.7), this corresponds to the choice of $w_E^{(n)}(x, y) = w_E(x, y)$ and $n w_I^{(n)}(x, y) = \beta(x)\theta(y)$. In the general form $n w_E^{(n)}(x, y)w_I^{(n)}(x, y)$, the factor $n w_I^{(n)}(x, y)$ may not only encompass effects that involve each member of the pair separately (as the ones captured by $\theta(y)$ and $\beta(x)$), but also effects that are more specific to the interaction between these pairs of individuals.

Remark 2.5 (Uniform scaling). Among the cases covered by Assumption 2.3-(iii), it is natural to distinguish the situations where the density of the graph is uniform over the feature interactions. Denoting by ϵ_n a scaling parameter, we consider next the cases where $w_I^{(n)} = \epsilon_n \bar{w}_I$ and $w_E^{(n)} = (n\epsilon_n)^{-1} \bar{w}_E$ for some functions \bar{w}_E, \bar{w}_I on \mathbb{X}^2 , so that, thanks to (2.7), $w^{(n)} = w$ with $w = \bar{w}_E \bar{w}_I$. Among the different possibilities for the scaling parameter ϵ_n , the case where $\epsilon_n = n^{-a+1}$ for some $a \in [1, 2]$ appears as the most characteristic to describe the level of sparsity of the graph, as the

total number of edges in the graph is then of order n^a . As n gets large, the number of contacts of an individual with feature x is well-described by the quantity $n \int_{\mathbb{X}} w_E^{(n)}(x, y) \mu(dy)$. The three interesting regimes are summed up in the following table.

	a	Nb. of contacts	Conn. density $w_E^{(n)}$	Inf. rate $w_I^{(n)}$
Dense graph	$a = 2$	n	1	n^{-1}
Sparse graphs	$a \in (1, 2)$	n^{a-1}	n^{a-2}	$n^{-(a-1)}$
Very sparse graphs	$a = 1$	1	n^{-1}	1

The most standard homogeneous case corresponds to the complete graph, corresponding to $w_E^{(n)} \equiv 1$. Note that in the dense and sparse case, the infection rate $w_I^{(n)}$ vanishes in the large n limit, but it is not the case in the very sparse case.

Notice that the sequence of graph realizations $(G^{(n)})_{n \in \mathbb{N}^*}$ converges to the graphon prescribed by \bar{w}_E only in the dense graphs case. For the sparse graphs case, there is already a limiting description of this sequence of graphs in terms of the subsampling of the graphon prescribed by \bar{w}_E , by expressing the graph as a kernel on a functional space (see [APSS20, Theorem 1]). By contrast, in the limiting *very sparse* case, where $a = 1$, there is local convergence of the graph towards a graph with finite degrees, whose realization brings an additional level of heterogeneity (as introduced in [BS01] see also [Bor16, Chap. 3] or [vdH24, Chap. 2]).

Aside from the structural condition, we also consider a crucial condition which ensures the convergence of the individual stochastic models to the same deterministic model as in the mean-field case. In order to state it, let us denote by $\mathcal{I}_n(g)$ the empirical average of a function g over all pairs of features:

$$\mathcal{I}_n(g) = \frac{1}{n^2} \mathbb{E} \left[\sum_{i, j \in \llbracket 1, n \rrbracket} g(x_i^{(n)}, x_j^{(n)}) \right] = \mathbb{E} \left[\int g d\mu^{(n)} \otimes d\mu^{(n)} \right]. \quad (2.9)$$

Assumption 2.6 (On the infection rate). The average infection rate vanishes when n goes to infinity:

$$\lim_{n \rightarrow \infty} \mathcal{I}_n(w_I^{(n)} \wedge 1) = 0, \quad \text{with } \mathcal{I}_n \text{ defined by (2.9).}$$

We are now ready to present our main result. Recall that $\mathcal{D} = \mathcal{D}(\mathbb{R}_+, \mathcal{M}_1)$ denotes the space of càd-làg paths from \mathbb{R}_+ to $\mathcal{M}_1 = \mathcal{M}_1(\mathbb{X} \times \{S, I\})$, and it is endowed with the Skorokhod topology.

Theorem 2.7 (Convergence of the stochastic individual-based model). *Let $\gamma^{(n)}$, $w_E^{(n)}$, $w_I^{(n)}$, γ , w and $\eta_0^{(n)}$ be such that Assumptions 2.3 and 2.6 are satisfied.*

Then, the sequence $(\eta^{(n)})_{n \in \mathbb{N}^}$ converges in probability in the Skorokhod space \mathcal{D} , to the continuous process $(\eta_t)_{t \in \mathbb{R}^+}$ with deterministic evolution defined by:*

$$\eta_t(dx, de) = \mu(dx) ((1 - u(t, x)) \delta_S(de) + u(t, x) \delta_I(de)), \quad (2.10)$$

where μ is the marginal of η_0 on \mathbb{X} , see (2.8), and where $(u(t, x))_{t \in \mathbb{R}_+, x \in \mathbb{X}}$ is the unique solution of the integro-differential equation:

$$\partial_t u(t, x) = (1 - u(t, x)) \int_{\mathbb{X}} u(t, y) w(x, y) \mu(dy) - \gamma(x) u(t, x), \quad (2.11)$$

with initial condition $u(0, \cdot) = u_0$, see (2.8).

Let us comment on the limit process. For $t \in \mathbb{R}_+$ and $x \in \mathbb{X}$, the value of $u(t, x)$ represents the probability for an individual with feature x to be infected at time t . The non-negative recovery rate function γ gives the rate at which individuals with feature x are recovering. The transmission kernel density function $w(x, y)$ captures in this expression the contribution to the infection rate of (susceptible) individuals with feature x due to individuals with feature y , scaled by the proportion of infected individuals with this feature, given by $u(t, y) \mu(dy)$. Properties of (2.11) have been studied in [DDZ22], while here we provide an interpretation of this equation as the large-population limit of a stochastic individual-based model. We refer to Section 3.4 for further comments.

Remark 2.8 (Examples of admissible uniform scaling). Consider the situation of Remark 2.5 where $w_I^{(n)} = \epsilon_n \bar{w}_I$ and $w_E^{(n)} = (n\epsilon_n)^{-1} \bar{w}_E$ with some bounded functions \bar{w}_E, \bar{w}_I on \mathbb{X}^2 and a uniform scaling parameter ϵ_n , so that Assumption 2.3-(iii) holds. Assumption 2.6 is then restated as $\lim_{n \rightarrow \infty} \epsilon_n = 0$, thus covering the cases of dense and sparse (but not very sparse) graphs.

This is no longer the case for the very sparse graphs model where $a = 1$ and $\epsilon_n = 1$. As we shall see in Subsection 4.3, when the graph is too sparse, meaning that $w_I^{(n)}$ is too large, we cannot expect the process $\eta^{(n)}$ to behave as the solution η to the problem (2.10). Let us mention that the very sparse graphs models encompass for example the configuration models with fixed degree distributions in large populations, which have been treated specifically in the case of SIR epidemics in various papers (e.g. [And99, BN08, BR13, DDMT12, JLW14, Mil11, Vol08]).

Remark 2.9 (Example of the SBM in the dense graphs setting). We cover in particular the dense Stochastic Block Model (SBM) with finite feature space, see Remark 2.1-(iii) on the SBM and Remark 2.8 for the uniform scaling with $a = 2$ and thus $\epsilon_n = 1/n$. With the notation therein, any individual with feature $q \in \llbracket 1, k \rrbracket$ recovers at rate $\gamma^{(n)}(q) = \gamma^q$ and is linked to any individual with feature r with probability $w_E^{(n)}(q, r) = w_E^{q,r} \geq 0$ (independently between the pairs), triggering the transmission of the disease to the individuals with feature q at rate $w_I^{(n)}(q, r) = w_I^{q,r}/n \geq 0$. Under the conditions of Theorem 2.7, the limiting process $(\eta_t)_{t \in \mathbb{R}_+}$ has a density with respect to the probability measure $\mu(dx) = \sum_{q \leq k} \mu_q \delta_q(dx)$ on $\mathcal{M}_1(\mathbb{X})$, where μ_q is the relative size of the population with feature q . The measure η_t is thus captured through the proportion u_t^q of infected individuals among the ones with feature q at time t , with the vector $(u_t^q)_{q \in \llbracket 1, k \rrbracket}$ satisfying the following system of k ODEs:

$$\partial_t u_t^q = (1 - u_t^q) \sum_{r=1}^k w_I^{q,r} w_E^{q,r} u_t^r \mu_r - \gamma^q u_t^q \quad \text{for } t \geq 0 \text{ and } q \in \llbracket 1, k \rrbracket.$$

Remark 2.10 (Comparison with [KHT22]). In [KHT22], it is clear that our Assumptions 2.3 and 2.6 are satisfied. We also consider more general initial conditions and do not restrict to $\mathbb{X} = [0, 1]$, which impacts the regularity conditions that one may consider for the parameter functions. Contrary to [KHT22], our framework allows to consider graphs that strongly exploit the geometry of the latent space \mathbb{X} , notably geometric graphs, see Remark 2.1-(ii) where $w(x, y) = g(|x - y|)$ with any function $g : \mathbb{R}_+ \mapsto \mathbb{R}_+$ having at most countably many discontinuities.

In [KHT22], the infection rate (per edge) takes a constant value that only depends on the population size n , and the recovery rate is constant $\gamma(x) \equiv 1$. This does not allow the dependence on the individual features, which might be of practical interest and insightful concerning the robustness of the results.

Lastly, it is assumed in [KHT22] that, in our notation, $w_E^{(n)}(x, y) = \kappa_n w(x, y)$ for some sequence κ_n , so that $w_I^{(n)}(x, y) \equiv 1/(n\kappa_n)$ and $\mathcal{I}_n(w_I^{(n)} \wedge 1) = [(n\kappa_n) \vee 1]^{-1}$. Their assumption that $\log(n)/(n\kappa_n) \rightarrow 0$ can, according to Assumption 2.6, be relaxed to $1/(n\kappa_n) \rightarrow 0$. Let us observe that, based on our Theorem 2.7, $w_I^{(n)}$ (and more precisely $\mathcal{I}_n(w_I^{(n)} \wedge 1)$) is the right quantity to control the convergence. The importance of the crucial condition involving $w_I^{(n)}$ is confirmed by the simulations that we present in Section 4. \square

3 Proof of Theorem 2.7

The proof of Theorem 2.7 follows a classical scheme. We establish the uniform tightness of the distributions of the processes $(\eta^{(n)})_{n \in \mathbb{N}^*}$ in Section 3.2, see Proposition 3.2. By Prohorov's theorem [Bil99, Theorems 5.1 and 5.2 p.59-60], this implies that this sequence of distributions is relatively compact. We then show in Section 3.3 that any potential limit must be solution to a measure-valued equation (3.15), see Proposition 3.5. This step requires a careful coupling between the processes $\eta^{(n)}$ and auxiliary processes $\tilde{\eta}^{(n)}$ on the complete graph but with modified infection rate. Using the uniqueness of the solution to Equation (3.15), see Lemma 3.7, we can conclude that there exists a unique limiting value to the sequence $(\eta^{(n)})_{n \in \mathbb{N}^*}$ and hence that it converges to the unique solution to Equation (3.15), say $\eta = (\eta_t)_{t \in \mathbb{R}_+}$. From the uniqueness of the solution to Equation (3.15), we will also establish in Lemma 3.7 that the measures η_t have densities with respect to $\mu \otimes (\delta_S + \delta_I)$ that satisfy (2.10)-(2.11). This will conclude the proof of Theorem 2.7.

Before entering the proofs of Propositions 3.2-3.5 and Lemma 3.7, we provide some results on the individual-based processes $\eta^{(n)}$ that will be used later. In particular, we will rely heavily on the stochastic differential equation (SDE) satisfied by these processes.

3.1 Stochastic differential equation for the individual-based model

In this section, we construct the graphs $G^{(n)}$ on a single probability space, and the processes $\eta^{(n)}$, for any $n \in \mathbb{N}^*$, as solutions of SDEs driven by Poisson point measures that do not depend on n nor on the graphs $G^{(n)}$. This pathwise construction allows us on the one hand to use tools from stochastic calculus for jump processes (see *e.g.* [IW89, Chapter II]), and on the other hand to couple $\eta^{(n)}$ with $\tilde{\eta}^{(n)}$ by constructing them on the same probability space with the same Poisson point measures.

Construction of the initial condition of the epidemic process. For $n \in \mathbb{N}^*$, let $\mathcal{X}^{(n)} = (x_i^{(n)})_{i \in \llbracket 1, n \rrbracket}$ be a sequence of random variables taking values in \mathbb{X} and let $\mathcal{E}^{(n)} = (E_0^{(n), i})_{i \in \llbracket 1, n \rrbracket}$ be a sequence of random variables taking values in $\{S, I\}$. For simplicity, we shall write x_i and E_0^i for $x_i^{(n)}$ and $E_0^{(n), i}$ when there is no ambiguity. The initial condition $\eta_0^{(n)}$ is then given by (2.3).

Construction of the random graphs $G^{(n)}$. Let $\mathcal{V} = (V(i, j))_{1 \leq i < j}$ be a family of independent uniform random variables on $[0, 1]$, and independent of $\mathcal{X}^{(n)}$ and $\mathcal{E}^{(n)}$. For convenience set $V(j, i) = V(i, j)$ and $V(i, i) = 0$. The graph $G^{(n)} = (V^{(n)}, E^{(n)})$ has vertices $V^{(n)} = \llbracket 1, n \rrbracket$ and the edge (i, j) belongs to $E^{(n)}$ if $V(i, j) \leq w_E^{(n)}(x_i, x_j)$.

Definition of the Poisson point measures. The state transitions are encoded thanks to the two following Poisson point measures, that are independent of \mathcal{V} , $\mathcal{X}^{(n)}$ and $\mathcal{E}^{(n)}$. (For Poisson point measures, we refer for example to [PB19, Part I, Appendix A.2]). Let $n(di)$ be the counting measure on \mathbb{N}^* .

1. For recovery events, we consider a Poisson point measure $Q_R(ds, di, du)$ on $\mathbb{R}_+ \times \mathbb{N}^* \times \mathbb{R}_+$, with intensity $ds n(di) du$. Each of its atom, say (s, i, u) , is a possible recovery event for the individual i at time s . The marker u allows to define whether the possible event really occurs or not. On the event:

$$A^{(n)}(i, u, s) = \{i \leq n\} \cap \{u \leq \gamma^{(n)}(x_i)\} \cap \{E_{s-}^i = I\}, \quad (3.1)$$

the recovery of individual i occurs at time s , otherwise nothing happens. By this acceptance-rejection method, we can ensure that recoveries for i occur at rate $\gamma^{(n)}(x_i)$ as long as i is infected.

2. For infection events, we consider a Poisson point measure $Q_I(ds, di, dj, du)$ on $\mathbb{R}_+ \times \mathbb{N}^* \times \mathbb{N}^* \times \mathbb{R}_+$, with intensity $ds \mathfrak{n}(di) \mathfrak{n}(dj) du$. Each of its atom, say (s, i, j, u) , is a possible infection event of individual i by individual j at time s . The marker u serves for the acceptance-rejection method to ensure that infection happens at rate $w_I^{(n)}(x_i, x_j)$ as long as j is infected and i susceptible and connected. On the event:

$$B^{(n)}(i, j, u, s) = \{i, j \leq n\} \cap C^{(n)}(i, j, u, s) \cap \{E_{s-}^i = S; E_{s-}^j = I\}, \quad (3.2)$$

where

$$C^{(n)}(i, j, u, s) = \{i \sim j\} \cap \{u \leq w_I^{(n)}(x_i, x_j)\}, \quad (3.3)$$

the individual i is infected by j , otherwise nothing happens. Notice the event $\{i \sim j\}$ can also be written $\{V(i, j) \leq w_E^{(n)}(x_i, x_j)\}$.

To simplify notation, the implicit parameters of the Poisson point measures are not recalled in the notation and we will use the following abbreviations:

$$dQ_R = Q_R(ds, di, du) \quad \text{and} \quad dQ_I = Q_I(ds, di, dj, du).$$

Encoding of $\eta^{(n)}$. The evolution of $\eta^{(n)}$ is given by the following equation, for $t \geq 0$:

$$\begin{aligned} \eta_t^{(n)} - \eta_0^{(n)} &= n^{-1} \int \mathbb{1}_{\{s < t\}} (\delta_{(x_i, S)} - \delta_{(x_i, I)}) \mathbb{1}_{A^{(n)}(i, u, s)} dQ_R \\ &\quad + n^{-1} \int \mathbb{1}_{\{s < t\}} (\delta_{(x_i, I)} - \delta_{(x_i, S)}) \mathbb{1}_{B^{(n)}(i, j, u, s)} dQ_I. \end{aligned} \quad (3.4)$$

Semi-martingale decomposition. We denote by $(\mathcal{F}_t^{(n)})_{t \in \mathbb{R}_+}$ the natural filtration associated to the Poisson point measures Q_R and Q_I , and the random variables \mathcal{V} , $\mathcal{X}^{(n)}$ and $\mathcal{E}^{(n)}$, so that the $V_{(i, j)}$'s, the x_i 's and the E_0^i 's are $\mathcal{F}_0^{(n)}$ -measurable. For any bounded measurable function f defined on $\mathbb{X} \times \{S, I\}$, we have the following semi-martingale decomposition of the real-valued process $(\langle \eta_t^{(n)} | f \rangle)_{t \in \mathbb{R}_+}$:

$$\langle \eta_t^{(n)} | f \rangle - \langle \eta_0^{(n)} | f \rangle = V_t^{(n)} + M_t^{(n)}, \quad (3.5)$$

where the predictable finite variation process $V^{(n)} = (V_t^{(n)})_{t \in \mathbb{R}_+}$ is given by:

$$\begin{aligned} V_t^{(n)} &= \int_0^t ds \int_{\mathbb{X}} \eta_s^{(n)}(dx, I) \gamma^{(n)}(x) (f(x, S) - f(x, I)) \\ &\quad + n^{-1} \int_0^t ds \sum_{i \sim j; i, j \in [1, n]} w_I^{(n)}(x_i, x_j) \mathbb{1}_{\{E_s^i = S, E_s^j = I\}} (f(x, I) - f(x, S)). \end{aligned} \quad (3.6)$$

The square integrable martingale process $M^{(n)} = (M_t^{(n)})_{t \in \mathbb{R}_+}$ is given by:

$$\begin{aligned} M_t^{(n)} &= n^{-1} \int \mathbb{1}_{\{s < t\}} (f(x_i, S) - f(x_i, I)) \mathbb{1}_{A^{(n)}(i, u, s)} d\tilde{Q}_R \\ &\quad + n^{-1} \int \mathbb{1}_{\{s < t\}} (f(x_i, I) - f(x_i, S)) \mathbb{1}_{B^{(n)}(i, j, u, s)} d\tilde{Q}_I, \end{aligned} \quad (3.7)$$

where \tilde{Q}_R and \tilde{Q}_I are the compensated measures of Q_R and Q_I respectively. Its quadratic variation $\langle M^{(n)} \rangle = (\langle M^{(n)} \rangle_t)_{t \in \mathbb{R}_+}$ is given by:

$$\begin{aligned} \langle M^{(n)} \rangle_t &= n^{-1} \int_0^t ds \int_{\mathbb{X}} \eta_s^{(n)}(dx, I) \gamma^{(n)}(x) \cdot (f(x, S) - f(x, I))^2 \\ &\quad + n^{-2} \int_0^t ds \sum_{i \sim j; i, j \in \llbracket 1, n \rrbracket} w_I^{(n)}(x_i, x_j) \mathbb{1}_{\{E_s^i = S, E_s^j = I\}} (f(x_i, I) - f(x_i, S))^2. \end{aligned} \quad (3.8)$$

For the complete graph, the above expressions can be simplified using (2.7) as follows.

Lemma 3.1 (The particular case of the complete graph). *When $w_E^{(n)} \equiv 1$ and using (2.7), Equations (3.6) and (3.8) become:*

$$\begin{aligned} V_t^{(n)} &= \int_0^t ds \int_{\mathbb{X}} \eta_s^{(n)}(dx, I) \gamma^{(n)}(x) \cdot (f(x, S) - f(x, I)) \\ &\quad + \int_0^t ds \int_{\mathbb{X}} \eta_s^{(n)}(dx, S) \int_{\mathbb{X}} \eta_s^{(n)}(dy, I) w^{(n)}(x, y) \cdot (f(x, I) - f(x, S)), \end{aligned} \quad (3.9)$$

and

$$\begin{aligned} \langle M^{(n)} \rangle_t &= n^{-1} \int_0^t ds \int_{\mathbb{X}} \eta_s^{(n)}(dx, I) \gamma^{(n)}(x) \cdot (f(x, S) - f(x, I))^2 \\ &\quad + n^{-1} \int_0^t ds \int_{\mathbb{X}} \eta_s^{(n)}(dx, S) \int_{\mathbb{X}} \eta_s^{(n)}(dy, I) w^{(n)}(x, y) \cdot (f(x, I) - f(x, S))^2. \end{aligned} \quad (3.10)$$

3.2 Tightness

The following tightness criterion relies on the semi-martingale decomposition given in the previous section. Recall that a sequence of random elements of \mathcal{D} is C-tight if it is tight with all the possible limits being a.s. continuous.

Proposition 3.2 (Tightness). *Under Assumption 2.3, the sequence of distributions of the processes $(\eta^{(n)})_{n \in \mathbb{N}^*}$ is C-tight on the Skorokhod space \mathcal{D} .*

In order to justify the tightness, we will have to specify global upper-bounds on the jump rate, which we relate to the initial condition $\eta_0^{(n)}$, and more precisely on its marginal on \mathbb{X} given by $\mu^{(n)}(dx) = \eta_0^{(n)}(dx, \{S, I\})$, see (2.5). (Notice that the measure $\mu^{(n)}$ is also the marginal on \mathbb{X} of $\eta_t^{(n)}$ for all $t \in \mathbb{R}_+$).

We consider the following non-negative function of $\mathcal{X}^{(n)}$:

$$\mathcal{J}^{(n)} = \frac{1}{n} \sum_{i, j \in \llbracket 1, n \rrbracket; i \sim j} w_I^{(n)}(x_i, x_j). \quad (3.11)$$

The terms $\mathcal{J}^{(n)}$ are potentially of order n since there can be up to n^2 terms in the sum. The next lemma asserts that their distributions are tight. By Assumption 2.3-(iii), there exist a finite positive constant C_w and an integer $n_0 \in \mathbb{N}^*$ large enough such that $\sup_{n \geq n_0} \|w^{(n)}\|_\infty \leq C_w$ and $\|w\|_\infty \leq C_w$. Without loss of generality, we can assume that $n_0 = 1$.

Lemma 3.3. *Under Assumption 2.3-(iii), we have:*

$$\mathbb{E}[\mathcal{J}^{(n)}] \leq C_w \quad (3.12)$$

and the sequence of distributions of $(\mathcal{J}^{(n)})_{n \in \mathbb{N}^*}$ is tight on \mathbb{R} .

Proof. According to the definition of the random graph of interactions, we have $i \sim j$ if $V(i, j) \leq w_E^{(n)}(x_i, x_j)$, where the $V(i, j)$ are sampled independently. Thus, we get:

$$\mathbb{E}[\mathcal{J}^{(n)} | \mathcal{X}^{(n)}] = \frac{1}{n} \sum_{i, j \leq n} w_I^{(n)}(x_i, x_j) \mathbb{P}(V(i, j) \leq w_E^{(n)}(x_i, x_j)) = \frac{1}{n^2} \sum_{i, j \leq n} w^{(n)}(x_i, x_j) \leq C_w.$$

Thanks to the Markov inequality since $\mathcal{J}^{(n)}$ is non-negative, we deduce that $\mathbb{P}(|\mathcal{J}^{(n)}| > C_w/\varepsilon) < \varepsilon$ for all $\varepsilon > 0$ and $n \in \mathbb{N}^*$. This gives the result. \square

We are now ready to prove Proposition 3.2.

Proof of Proposition 3.2. Let D_0 be a fixed set of real-valued continuous bounded functions defined on $\mathbb{X} \times \{S, I\}$, containing the constant functions, and assume that D_0 is separating, that is:

$$(\forall f \in D_0, \forall \nu, \nu' \in \mathcal{M}_1, \langle \nu, f \rangle = \langle \nu', f \rangle) \implies \nu = \nu'.$$

According to Theorem II.4.1 in [Per99], the sequence of processes $(\eta^{(n)})_{n \in \mathbb{N}^*}$ is C-tight in \mathcal{D} if and only if:

- (a) **Compact Containment Condition (CCC).** For all $\varepsilon > 0$, $T > 0$, there exists a compact set $K_{T, \varepsilon}$ in $\mathbb{X} \times \{S, I\}$ such that:

$$\sup_{n \in \mathbb{N}^*} \mathbb{P} \left(\sup_{t \leq T} \eta_t^{(n)}(K_{T, \varepsilon}^c) > \varepsilon \right) < \varepsilon.$$

- (b) **Tightness of the projections.** For all $f \in D_0$, the sequence $(\langle \eta^{(n)}, f \rangle)_{n \in \mathbb{N}^*}$ is C-tight in $\mathcal{D}(\mathbb{R}_+, \mathbb{R})$.

We first prove the compactness property (a). According to Assumption 2.3-(ii), the random sequence $(\eta_0^{(n)})_{n \in \mathbb{N}^*}$ converges in distribution to η_0 (in \mathcal{M}_1 endowed with the topology of the weak convergence). Recall $\mu^{(n)}$ is the marginal of $\eta_0^{(n)}$ on \mathbb{X} , see (2.5); and μ is the marginal of η_0 on \mathbb{X} , see (2.8). We deduce that the random sequence $(\mu^{(n)})_{n \in \mathbb{N}^*}$ converges weakly and in distribution to μ (in $\mathcal{M}_1(\mathbb{X})$). Since $\mathcal{M}_1(\mathbb{X})$ is a Polish space, Prohorov's theorem implies that this sequence is tight, and thus, for all $\varepsilon > 0$, there is a compact set K_ε in \mathbb{X} such that:

$$\sup_{n \in \mathbb{N}^*} \mathbb{P} \left(\mu^{(n)}(K_\varepsilon^c) > \varepsilon \right) < \varepsilon.$$

Since the marginal on \mathbb{X} of $\eta_t^{(n)}$ is also $\mu^{(n)}$, we deduce (a) with the compact set $K_\varepsilon \times \{S, I\}$:

$$\sup_{n \in \mathbb{N}^*} \mathbb{P} \left(\eta_t^{(n)}(K_\varepsilon^c \times \{S, I\}) > \varepsilon \text{ for all } t \in \mathbb{R}_+ \right) < \varepsilon.$$

We now prove (b) on the tightness of the projections. By Assumption 2.3-(iv), there exists a finite positive constant C_γ and $n_0 \in \mathbb{N}^*$ large enough such that $\sup_{n \geq n_0} \|\gamma^{(n)}\|_\infty \leq C_\gamma$ and $\|\gamma\|_\infty \leq C_\gamma$. Without loss of generality, we can assume that $n_0 = 1$.

We consider the processes $\tilde{V}^{(n)} = (\tilde{V}_t^{(n)})_{t \in \mathbb{R}_+}$ and $\tilde{A}^{(n)} = (\tilde{A}_t^{(n)})_{t \in \mathbb{R}_+}$ defined by:

$$\tilde{V}_t^{(n)} = 2\|f\|_\infty(C_\gamma + \mathcal{J}^{(n)})t \quad \text{and} \quad \tilde{A}_t^{(n)} = \frac{4}{n}\|f\|_\infty^2(C_\gamma + \mathcal{J}^{(n)})t. \quad (3.13)$$

Thanks to Lemma 3.3, we deduce that the sequences of processes $(\tilde{V}^{(n)})_{n \in \mathbb{N}^*}$ and $(\tilde{A}^{(n)})_{n \in \mathbb{N}^*}$ are C-tight in $\mathcal{D}(\mathbb{R}_+, \mathbb{R})$ (as they are tight with all the possible limits being a.s. continuous). Following [JS87, Section VI.3], we say that a non-negative non-decreasing, right-continuous and null at 0 process is an “increasing process”. Let $\text{Var}(V^{(n)})$ denote the variation process of $V^{(n)}$ defined in (3.6). Since $\eta^{(n)}$ is a probability measure, we deduce that the process $\tilde{V}^{(n)} - \text{Var}(V^{(n)})$ is an increasing process. Thanks to (3.8), the process $\tilde{A}^{(n)} - \langle M^{(n)} \rangle$ is also an increasing process. We deduce from Propositions VI.3.35 in [JS87] that the sequences $(\text{Var}(V^{(n)}))_{n \in \mathbb{N}^*}$ and $(\langle M^{(n)} \rangle)_{n \in \mathbb{N}^*}$ are C-tight. Then, we deduce from Propositions VI.3.36 therein that the sequence $(V^{(n)})_{n \in \mathbb{N}^*}$ is C-tight. Since the sequence $(\eta_0^{(n)})_{n \in \mathbb{N}^*}$ is tight thanks to Assumption 2.3-(ii), we also deduce from Theorem VI.4.13 therein that the sequence $(\eta_0^{(n)} + M^{(n)})_{n \in \mathbb{N}^*}$ is tight. Then use Corollary VI.3.33 therein to deduce that the sequence $(\eta^{(n)} = \eta_0^{(n)} + V^{(n)} + M^{(n)})_{n \in \mathbb{N}^*}$ is tight.

Eventually, notice that the sequence $(\tilde{A}^{(n)})_{n \in \mathbb{N}^*}$ converges to 0, which implies that the sequence $(\langle M^{(n)} \rangle)_{n \in \mathbb{N}^*}$ and thus the sequence $(M^{(n)})_{n \in \mathbb{N}^*}$ converge also to 0 a.s. and in L^1 uniformly for $t \in [0, T]$, T finite. Since $(V^{(n)})_{n \in \mathbb{N}^*}$ is C-tight, we also deduce that $(\langle \eta^{(n)}, f \rangle)_{n \in \mathbb{N}^*}$ is C-tight. Then take for D_0 the set of bounded continuous measurable functions defined on $\mathbb{X} \times \{S, I\}$ to deduce that (b) holds.

We deduce from [Per99, Theorem II.4.1] that the sequence $(\eta^{(n)})_{n \in \mathbb{N}^*}$ is C-tight in \mathcal{D} . \square

As a by-product of the above proof, we get the following result.

Corollary 3.4. *Suppose the assumptions of Proposition 3.2 hold. Let f be a bounded measurable function defined on $\mathbb{X} \times \{S, I\}$. Then, the sequence of martingales $(M^{(n)})_{n \in \mathbb{N}^*}$ defined by (3.7), is such that for all $T \in \mathbb{R}_+$:*

$$\lim_{n \rightarrow \infty} \mathbb{E} \left[\sup_{t \in [0, T]} \left(M_t^{(n)} \right)^2 \right] = 0.$$

Proof. At the end of the proof of Proposition 3.2, we get that $\langle M^{(n)} \rangle_t \leq \tilde{A}_t^{(n)}$, with $\tilde{A}^{(n)}$ defined in (3.13). Then use Doob’s inequality for the square integrable martingale $M^{(n)}$ and (3.12) to conclude. \square

3.3 Identification of the equation characterizing the limiting values

Under the hypotheses of Proposition 3.2, the sequence $(\eta^{(n)})_{n \in \mathbb{N}^*}$ is C-tight in \mathcal{D} . Let $\bar{\eta} = (\bar{\eta}_t)_{t \in \mathbb{R}_+} \in \mathcal{D}$ be a possible limit in distribution. In particular, the function $t \mapsto \bar{\eta}_t$ is continuous.

By construction, we have that $\eta_t^{(n)}(dx \times \{S, I\})$ is equal to $\mu^{(n)}$, see (2.5) for all $t \in \mathbb{R}_+$. According to Assumption 2.3-(ii), the sequence $(\mu^{(n)})_{n \in \mathbb{N}^*}$ converges in distribution to μ . Since the map $\nu \mapsto \nu(dx \times \{S, I\})$ from \mathcal{M}_1 to $\mathcal{M}_1(\mathbb{X})$ is continuous, and since $\bar{\eta}$ is continuous in \mathcal{D} , we deduce that a.s.:

$$\bar{\eta}_t(dx \times \{S, I\}) = \mu(dx) \quad \text{for all } t \in \mathbb{R}_+. \quad (3.14)$$

We state in the next proposition that $\bar{\eta} \in \mathcal{D}$ is a (continuous) solution to:

$$\Psi_{f,t}(\nu) = 0 \quad \text{for all } t \in \mathbb{R}_+, \quad (3.15)$$

for any real-valued continuous bounded function f defined on $\mathbb{X} \times \{S, I\}$, where for $\nu = (\nu_t)_{t \in \mathbb{R}_+} \in \mathcal{D}$:

$$\begin{aligned} \Psi_{f,t}(\nu) = \langle \nu_t - \nu_0 | f \rangle &- \int_0^t dr \int_{\mathbb{X}} \nu_r(dx, I) \gamma(x) \cdot (f(x, S) - f(x, I)) \\ &- \int_0^t dr \int_{\mathbb{X}} \nu_r(dx, S) \int_{\mathbb{X}} \nu_r(dy, I) w(x, y) \cdot (f(x, I) - f(x, S)). \end{aligned} \quad (3.16)$$

Proposition 3.5 (Property of the limiting process). *Under Assumptions 2.3 and 2.6, any limiting value $\bar{\eta}$ of $(\eta^{(n)})_{n \in \mathbb{N}^*}$ in \mathcal{D} is a.s. continuous and solution of Equation (3.15).*

The rest of the section is devoted to the proof of Proposition 3.5. It is divided into several steps: first, we consider the case of a complete graph with $w_E^{(n)} \equiv 1$, second, in the heterogeneous case, we construct a coupling between the epidemic process $\eta^{(n)}$ and an epidemic process $\tilde{\eta}^{(n)}$ defined on the complete graph, but with a modified infection rate, third we end the proof.

Step 1: Limiting equation for the epidemic on the complete graph ($w_E^{(n)} \equiv 1$)

In this section, we assume that $w_E^{(n)} \equiv 1$. Thanks to Lemma 3.1, we get from (3.5) and (3.9) that:

$$\begin{aligned} \Psi_{f,t}(\eta^{(n)}) = M_t^{(n)} &+ \int_0^t dr \int_{\mathbb{X}} \eta_r^{(n)}(dx, S) \int_{\mathbb{X}} \eta_r^{(n)}(dy, I) (w^{(n)}(x, y) - w(x, y)) \cdot (f(x, I) - f(x, S)) \\ &+ \int_0^t dr \int_{\mathbb{X}} \eta_r^{(n)}(dx, I) (\gamma^{(n)}(x) - \gamma(x)) \cdot (f(x, S) - f(x, I)). \end{aligned}$$

By Assumption 2.3-(iii),(iv), the following upper-bound holds:

$$|\Psi_{f,t}(\eta^{(n)})| \leq |M_t^{(n)}| + 2t \|f\|_{\infty} (\|w^{(n)} - w\|_{\infty} + \|\gamma^{(n)} - \gamma\|_{\infty}).$$

Then use Corollary 3.4 and the uniform convergence of $\gamma^{(n)}$ and $w^{(n)}$ to γ and w to conclude that $\lim_{n \rightarrow \infty} \mathbb{E} \left[|\Psi_{f,t}(\eta^{(n)})| \right] = 0$.

Since the functions w and γ are continuous $\mu^{\otimes 2}$ -a.s. and μ -a.s. we deduce that the functional $\Psi_{f,t}$ is continuous at any $\nu \in \mathcal{D}$ such that $\nu_s(dx \times \{S, I\})$ is absolutely continuous with respect to μ for a.e. $s \in [0, t]$. Thanks to (3.14), a.s. for all $t \geq 0$ the probability measure $\bar{\eta}_t(dx \times \{S, I\})$ is absolutely continuous with respect to $\mu(dx)$. We deduce that $\Psi_{f,t}(\eta^{(n)})$ converges in distribution to $\Psi_{f,t}(\bar{\eta})$, and since $|\Psi_{f,t}(\eta^{(n)})| \leq 2\|f\|_{\infty} \cdot (1 + tC_w + tC_{\gamma})$, see (3.16), we deduce that $\lim_{n \rightarrow \infty} \mathbb{E} \left[|\Psi_{f,t}(\eta^{(n)})| \right] = \mathbb{E} \left[|\Psi_{f,t}(\bar{\eta})| \right]$. This concludes that $\mathbb{E} \left[|\Psi_{f,t}(\bar{\eta})| \right] = 0$, that is, $\bar{\eta}$ is a.s. solution of (3.15).

Step 2: Coupling for heterogeneous contact graphs ($w_E^{(n)} \neq 1$)

Now we consider the general case of the epidemic process $\eta^{(n)}$ associated to connection density $w_E^{(n)}$, infection rate $w_I^{(n)}$ and recovery rate $\gamma^{(n)}$. We shall couple the process $\eta^{(n)}$ with an epidemic process $\tilde{\eta}^{(n)}$ on a complete graph associated to connection density $\tilde{w}_E^{(n)} \equiv 1$, infection rate $\tilde{w}_I^{(n)} = w_I^{(n)} w_E^{(n)}$ and same recovery rate $\tilde{\gamma}^{(n)} = \gamma^{(n)}$. The two epidemic processes shall also start with the same initial condition $\eta_0^{(n)} = \tilde{\eta}_0^{(n)}$. The next proposition, whose technical proof is postponed to Section A, gives for a well chosen coupling an upper bound on the distance in variation between the two epidemic processes.

We denote by $\|\nu\|_{TV}$ the total variation norm of a signed measure on $\mathbb{X} \times \{S, I\}$. Recall the functional \mathcal{I}_n in (2.9).

Proposition 3.6 (A control using coupling). *Under Assumption 2.3, for all $T \geq 0$, there exists a finite constant C_T (independent of n) and a sequence of epidemic processes $(\tilde{\eta}^{(n)})_{n \in \mathbb{N}^*}$ on a complete graph (with $\tilde{\eta}^{(n)}$ associated to connection density $\tilde{w}_E^{(n)} \equiv 1$, infection rate $\tilde{w}_I^{(n)} = w_I^{(n)} w_E^{(n)}$, recovery rate $\tilde{\gamma}^{(n)} = \gamma^{(n)}$ and initial condition $\tilde{\eta}_0^{(n)} = \eta_0^{(n)}$) such that:*

$$\mathbb{E} \left[\sup_{t \in [0, T]} \|\eta_t^{(n)} - \tilde{\eta}_t^{(n)}\|_{TV} \right] \leq C_T \mathcal{I}_n(w_I^{(n)} \wedge 1).$$

We shortly explain how the auxiliary process $\tilde{\eta}^{(n)}$ is constructed. The graph $G^{(n)}$ on which the epidemic described by $\eta^{(n)}$ spreads is encoded by the random variables $(V(i, j))_{1 \leq i < j}$ of Section 3.1.

The dynamics of $\tilde{\eta}^{(n)}$ can be interpreted as the one for which this graph structure is initially the same (that is, encoded by the random variables $(V(i, j))_{1 \leq i < j}$) but then each edge involved in an infection event is resampled. This amounts to modifying the infection rate by multiplying it by the probability to get the edge, that is $\tilde{w}_I^{(n)} = w_I^{(n)} w_E^{(n)}$, and considering that the propagation holds on a complete graph.

Step 3: End of the proof

Suppose that the sequence $(\eta^{(n)})_{n \in \mathbb{N}^*}$, which is C-tight according to Proposition 3.2, converges in distribution along a sub-sequence $(n_k)_{k \in \mathbb{N}^*}$ towards a certain trajectory $\eta \in \mathcal{D}$. Thanks to Proposition 3.6 and Assumption 2.6, the sequence $(\tilde{\eta}^{(n_k)})_{k \in \mathbb{N}^*}$ (of epidemic process on complete graphs) converges also in distribution towards η . By Step 1, the limit η is solution to Equation (3.15). Thus, all the limiting values of the sequence $(\eta^{(n)})_{n \in \mathbb{N}^*}$ are solutions of Equation (3.15). This ends the proof of Proposition 3.5.

3.4 Uniqueness of the limit

We shall prove the existence and uniqueness of the solution of (3.15). The measurable non-negative functions w and γ defined respectively on \mathbb{X}^2 and \mathbb{X} are assumed to be bounded. We first comment on the existence and uniqueness of solution to the ODE (2.11) in the Banach space $(\mathcal{L}^\infty, \|\cdot\|_\infty)$ of bounded measurable functions defined on \mathbb{X} endowed with the supremum norm. Let $\Delta \subset \mathcal{L}^\infty$ be the set of non-negative functions bounded by 1. Under the further assumption that γ is positive, it is proved in [DDZ22, Section 2] that for an initial condition $u_0 \in \Delta$, the ODE (2.11) admits a unique (maximal) solution; it is defined on \mathbb{R}_+ and takes values in Δ . A careful reading of [DDZ22] provides that one can assume that γ is only non-negative without altering the results nor the proofs of Section 2 therein. Thus the solution $(u_t = (u(t, x))_{x \in \mathbb{X}})_{t \in \mathbb{R}_+}$ of (2.11) with initial condition $u_0 \in \Delta$ exists and is unique.

The continuous \mathcal{M}_1 -valued process $\eta = (\eta_t)_{t \in \mathbb{R}_+}$, with deterministic evolution, defined by (2.10) is clearly a solution of (3.15) for any continuous function f defined on $\mathbb{X} \times \{S, I\}$ with initial condition η_0 given by (2.8). We shall now prove the following uniqueness result.

Lemma 3.7 (Uniqueness for Equation (3.15)). *Assume the measurable non-negative functions w and γ defined respectively on \mathbb{X}^2 and \mathbb{X} are bounded. If $\bar{\eta} \in \mathcal{D}$ is a.s. a continuous process solution of (3.15) (for any real-valued continuous bounded function f defined on $\mathbb{X} \times \{S, I\}$) with initial condition η_0 given by (2.8), then a.s. $\bar{\eta} = \eta$.*

Proof. Let $\bar{\eta} \in \mathcal{D}$ be continuous and a solution of (3.15) with initial condition η_0 given by (2.8). Taking f such that $f(\cdot, S) = f(\cdot, I)$, we deduce from (3.15) that for all $t \in \mathbb{R}_+$ the marginals of $\bar{\eta}_t$ on \mathbb{X} are constant equal to the marginal of η_0 given by μ (see (2.8)). This implies that for all $t \in \mathbb{R}_+$,

the probability measure $\bar{\eta}_t$ is absolutely continuous with respect to $\mu \otimes (\delta_S + \delta_I)$, and thus:

$$\bar{\eta}(dx, de) = \mu(dx) ((1 - \bar{u}(t, x)) \delta_S(de) + \bar{u}(t, x) \delta_I(de)),$$

for some measurable function $\bar{u} = (\bar{u}_t = (u(t, x))_{x \in \mathbb{X}})_{t \in \mathbb{R}_+}$ taking values in $[0, 1]$. Let g be a real-valued continuous bounded function defined on \mathbb{X} and $t \in \mathbb{R}_+$. Taking $f(x, e) = g(x) \mathbb{1}_{\{e=I\}}$, we deduce from $\Psi_{f,t}(\bar{\eta}) = 0$ that $\int_{\mathbb{X}} g(x) \bar{U}_t(x) \mu(dx) = 0$ where:

$$\bar{U}_t(x) = \bar{u}_t(x) - u_0(x) - \int_0^t dr \left((1 - \bar{u}_r(x)) \int_{\mathbb{X}} \mu(dy) w(x, y) \cdot \bar{u}_r(y) - \gamma(x) \cdot \bar{u}_r(x) \right).$$

Since g and t are arbitrary, we deduce that $\bar{U}_t = 0$ μ -a.e. for all $t \in \mathbb{R}_+$. Using (2.11), we obtain that for all $t \in \mathbb{R}_+$:

$$\|\bar{u}_t - u_t\|_1 \leq (2C_w + C_\gamma) \int_0^t dr \|\bar{u}_r - u_r\|_1,$$

where $\|\cdot\|_1$ denotes the usual norm on $L^1(\mathbb{X}, \mu)$. By Grönwall's Lemma, we deduce that $\|\bar{u}_t - u_t\|_1 = 0$ for all $t \in \mathbb{R}_+$. This implies that for all $t \in \mathbb{R}_+$, μ -a.e. $\bar{u}_t = u_t$, that is $\bar{\eta}_t = \eta_t$ for all $t \in \mathbb{R}_+$. \square

4 Simulations and discussion

In this section, we will focus on the special case of an homogeneous population to illustrate our main convergence result and to highlight the crucial role of Assumption 2.6.

4.1 Simulations setup: Erdős–Rényi graph and homogeneous infection rate

We consider the Erdős–Rényi graph, which amounts to taking $w_E^{(n)}$ homogeneous over the population, and thus depending only on n , not on the feature. We consider an infection rate $w_I^{(n)}$ which is homogeneous over the population, too, so that $w^{(n)} = n w_E^{(n)} w_I^{(n)}$ is homogeneous and converges to a constant transmission kernel w . For simplicity, the initial condition u_0 is also taken to be constant. In this case, Equation (1.3) prescribes the density (identified with the proportion) of the infected population, now uniform over the features. We thus recover the classical SIS model introduced by Kermack and McKendrick (in [KM32, KM33], as a special case):

$$\partial_t u(t) = w \cdot (1 - u(t)) \cdot u(t) - \gamma \cdot u(t). \quad (4.1)$$

If $w = 0$, then there is asymptotically no propagation of the epidemics: our results also cover this degenerate case, which will not be considered further. Assuming that the model is not degenerate, that is $w > 0$, the most natural choice is setting $w^{(n)} = w$. For the resulting Erdős–Rényi graph $G^{(n)}$, edges in the graph of n vertices are thus kept with probability:

$$w_E^{(n)} = \frac{w}{n w_I^{(n)}}.$$

Assumption 2.6 corresponds to $\lim_{n \rightarrow \infty} w_I^{(n)} = 0$, that is, $\lim_{n \rightarrow \infty} n w_E^{(n)} = +\infty$. Notice that $n w_E^{(n)}$ is the expected number of neighbors (for any individual), which is purely a local quantity.

Remark 4.1 (Assumption 2.6 and connectivity). We compare the condition $\lim_{n \rightarrow \infty} n w_E^{(n)} = +\infty$ with the well-known connectivity properties of Erdős–Rényi graphs, which have a sharp connectivity threshold when $n w_E^{(n)}$ is around $\log n$ (see e.g. [vdH17, Theorem 5.8]). Erdős–Rényi graphs may

exhibit the so-called super-critical regime (see e.g. [vdH17, Section 4.4]): if $n w_E^{(n)} \geq c > 1$, with a probability that converges to 1 as n tends to infinity, then there exists a connected component, called the giant component, which contains a positive fraction of the n vertices, while the second-largest component has at most $O(\log n)$ vertices. Furthermore, if $n w_E^{(n)} \geq d \log(n)$, with a probability that converges to 1 as n tends to infinity, then there are only a giant component and isolated vertices if $d > 1/2$, and the graph is connected if $d > 1$ (see [vdH17, Section 5.3, Proposition 5.10 and Theorem 5.8]). Instead, in the super-critical regime with bounded $n w_E^{(n)}$, the size of the second largest component is of order $\log(n)$ (see [vdH17, Section 4.4]).

Based on this description, we can observe that Assumption 2.6 does not imply the graph to be connected. However, Assumption 2.6 implies that the graph is in the super-critical regime. At the same time, the super-critical regime also includes some graphs which we qualify of ‘very sparse’, where $n w_E^{(n)}$ is constant and hence Assumption 2.6 fails. We will consider the latter case in Sect. 4.3, and show that the mean-field approximation is not good in this regime. \square

For the simulations, we shall consider the numerical values $w = 3$ and $\gamma = 0.7$. The reproduction number is given by:

$$R_0 = \frac{w}{\gamma} \simeq 4.3.$$

Since $R_0 > 1$, we get that

$$\lim_{t \rightarrow \infty} u(t) = 1 - 1/R_0 =: u_*$$

and that $u(t) \approx u_* + C e^{-(R_0-1)t}$ for large t and some finite constant C , provided the initial condition $u(0)$ is positive. In particular, on the time-interval $I_0 = [20, 80]$, the function u is numerically constant and equal to the equilibrium u_* .

Let $u^{(n)}(t)$ denote the proportion of the infected population at time $t \geq 0$, that is, $u^{(n)}(t) = \eta_t^{(n)}(\mathbb{X}, I)$ in the terminology of Section 2.2. For the simulations, we use the Gillespie algorithm to sample exact trajectories (up to numerical limitations), with the initial population completely infected, that is, $u^{(n)}(0) = 1$.

Remark 4.2. As in general the asymptotic equilibrium is not unique (notably when the graph is not connected), starting from the initial condition $u_0 = 1$ shall provide the estimation on the asymptotic equilibrium that is maximal in terms of the infected proportion of individuals (cf [DDZ22], provided the stochasticity does not move the process away from it). As starting simulations with any positive initial conditions does not change the results significantly, we shall only consider $u_0 = 1$ as initial condition.

In the simulations we will either consider a fixed population size $n_0 = 2000$, or show plots for growing values of n . When studying the different sparsity regimes as in Remark 2.5, we will consider $w_E^{(n)} \asymp n^{a-2}$, which corresponds to $w_I^{(n)} \asymp n^{-a+1}$; for ease of notation, we will rather use the following parameter instead of a :

$$\alpha = a - 1 \geq 0 \quad \text{so that} \quad w_E^{(n)} \asymp n^{\alpha-1} \quad \text{and} \quad w_I^{(n)} \asymp n^{-\alpha},$$

in order to focus on the difference between the case $\alpha > 0$ (Assumption 2.6 holds) and the very sparse case $\alpha = 0$ (Assumption 2.6 fails). More precisely, in all plots concerning the asymptotic behavior $w_I^{(n)} \asymp n^{-\alpha}$ we will use the values

$$w_I^{(n)} = 1.2 (n/n_0)^{-\alpha}.$$

4.2 Numerical observation of the convergence

In this section, we illustrate how the solution u of (4.1) (or rather its equilibrium value $u_* =$

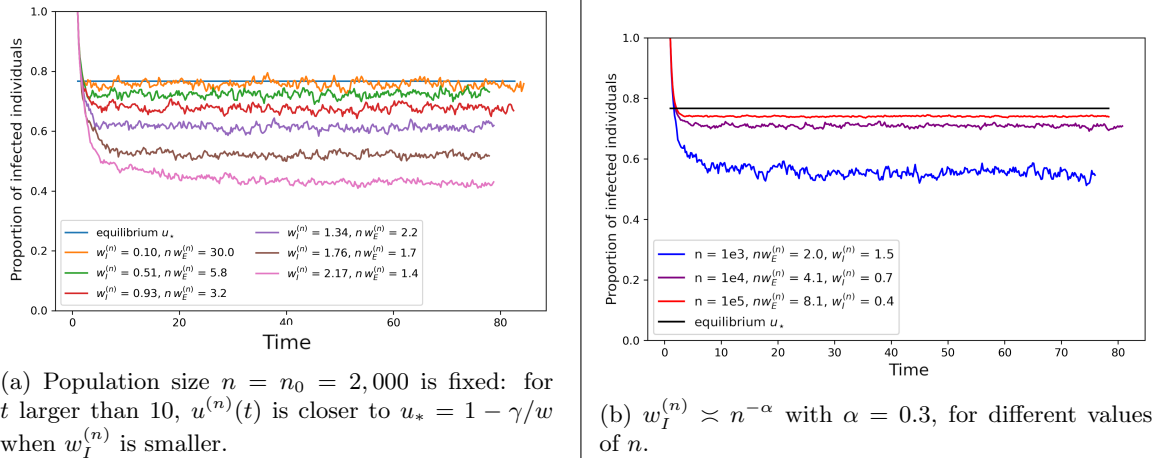


Figure 4.1: Evolution of $t \mapsto u^{(n)}(t)$ for different choices of $w_I^{(n)}$.

$\lim_{t \rightarrow \infty} u(t)$, which is attained by $u(t)$ within numerical precision for time $t \geq 20$) is a good approximation of $u^{(n)}$ whenever $w_I^{(n)}$ is small enough, consistently with the convergence of $u^{(n)}$ to u , for $n \rightarrow \infty$, if $w_I^{(n)} \rightarrow 0$ (i.e., Assumption 2.6 holds).

4.2.1 The proportion $u^{(n)}(t)$ of infected population and the limit u_*

In Fig. 4.1, we represent the evolution of $u^{(n)}(t)$ for $t \in [0, 80]$: each curve corresponds to a single run on one sampled graph. In the left panel, we consider a population of size $n = n_0$, with $n_0 = 2000$, and different values of $w_I^{(n)}$: as expected, one can clearly see that the deviation of $u^{(n)}$ from u_* is small, compared to the temporal fluctuations, when $w_I^{(n)}$ is close to 0.1 and increases to much higher values as $w_I^{(n)}$ grows closer to 2. In the right panel, we consider $w_I^{(n)} \asymp n^{-\alpha}$ for $\alpha = 0.3$ and different values of n : one can clearly see that the discrepancy is reduced as $w_I^{(n)}$ gets closer to 0. For $n = 10^5$, the temporal fluctuations are almost not visible on the plot, while the discrepancy with u_* is small but still noticeable.

Fig. 4.1 shows that, for large population size n , the trajectory of $u^{(n)}$ has small fluctuations, which seem much smaller than the discrepancy between $u^{(n)}$ and u_* . For this reason, we choose to investigate the temporal fluctuations of $u^{(n)}$, which can be interpreted as an internal variance term, in Section 4.2.2 and the discrepancy between a temporal average of $u^{(n)}$ and u_* , which can be interpreted as a bias term, in Section 4.2.3.

4.2.2 An internal noise: the temporal fluctuations of $u^{(n)}$ for large population size n

In order to measure the temporal fluctuations of the proportion of infected individuals, we compute the standard deviation of the data points in the time-interval $I_0 = [20, 80]$. More precisely, the random temporal average $\hat{u}_*^{(n)}$ and the corresponding standard deviation $\hat{\sigma}_n$ of $u^{(n)}$ over the time

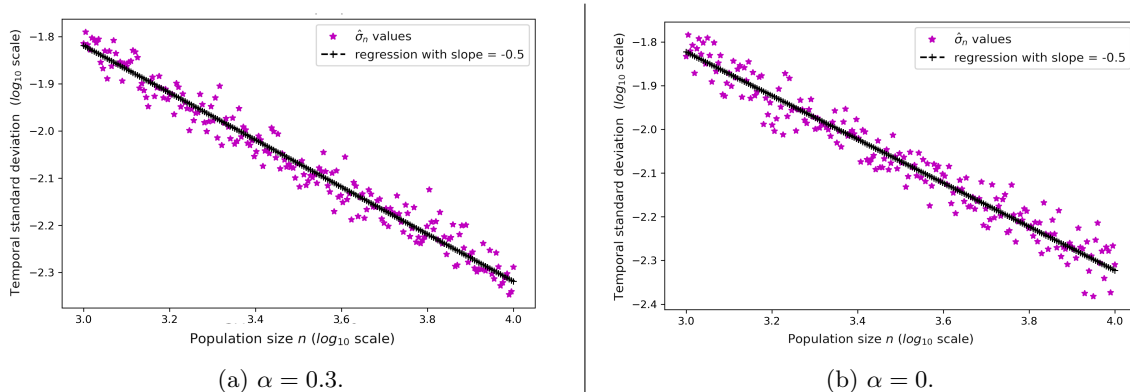


Figure 4.2: Temporal fluctuations: temporal standard deviation $\hat{\sigma}_n$ of the proportion of infected individuals (defined in (4.2)), and comparison with the decay $1/\sqrt{n}$, when $w_I^{(n)} \asymp n^{-\alpha}$. Each star point is obtained from a single run.

interval I_0 of length $|I_0| = 60$ are given by:

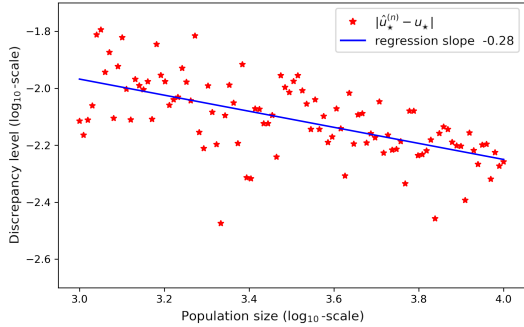
$$\hat{u}_*^{(n)} = \frac{1}{|I_0|} \int_{I_0} u^{(n)}(t) dt \quad \text{and} \quad \hat{\sigma}_n^2 = \frac{1}{|I_0|} \int_{I_0} \left(u^{(n)}(t) - \hat{u}_*^{(n)} \right)^2 dt. \quad (4.2)$$

This computation is motivated by the Orstein-Uhlenbeck description of the fluctuations in the compartmental SIS model, corresponding to $w_E^{(n)} = 1$, which are known to be of order $1/\sqrt{n}$ (see [PB19, Theorem 2.3.2]). In Fig. 4.2, we plot the temporal standard deviation $\hat{\sigma}_n$ as a function of the population size n . The resulting relation is compared to the prediction of the central limit theorem for mean-field interactions, that is a decay as $1/\sqrt{n}$. We consider the sparse case $\alpha = 0.3$ in the left panel, and the very sparse case $\alpha = 0$ (so that $w_I^{(n)} = 1.2$ for all n) in the right panel. The prediction of a decay as $1/\sqrt{n}$ is clearly confirmed, even in the very sparse case.

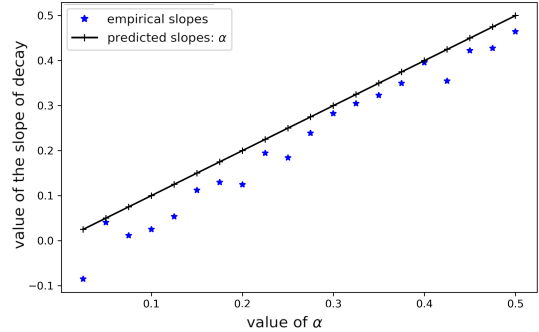
4.2.3 The bias of the temporal average of $u^{(n)}$ for different sparsity levels

To obtain more reliable estimations of the decay in the discrepancy between the random process $u^{(n)}$ and the equilibrium u_* , we focus in Fig. 4.3 on the discrepancy between the random temporal average $\hat{u}_*^{(n)}$ and u_* . In the left panel of Fig. 4.3, we thus plot the deviation $|\hat{u}_*^{(n)} - u_*|$ in a log-log scale as a function of population size n , for $\alpha = 0.3$. Each of the $N = 100$ points is obtained from a single run (with the same relation for $w_I^{(n)}$ as in Fig. 4.2). We then find the regression slope of such points, which turns out to be -0.28 , not far from $-\alpha = -0.3$.

In the right panel, we plot these decay slopes for different values of α . Each point in the right panel is an empirical regression slope of $|\hat{u}_*^{(n)} - u_*|$ in n with a log-log scale, obtained with the same procedure used in left panel for $\alpha = 0.3$, requiring $N = 100$ runs. Based on our analysis, we expect that $n^{-\alpha}$ is the maximal level of deviation that can be due to the graph structure, in view of the bias term in the coupling argument (see Proposition 3.6); whereas $1/\sqrt{n}$ is the internal fluctuations level in the martingale term (see Equation 3.5) that dominates the deviations in the mean-field case (see Fig. 4.2). Provided $\alpha < 0.5$, the bias term $n^{-\alpha}$ is large against the fluctuation term $1/\sqrt{n}$. This intuition is confirmed in the right panel of Fig. 4.3 where the empirical slopes are very close to a linear growth in α , so long as $\alpha \leq 0.5$. The quality of this approximation of linear growth is also quantified, as indicated in the legend, by the coefficient of determination $R^2 \approx 0.97$, very close to 1.



(a) $|\hat{u}_*^{(n)} - u_*|$ for growing population size n (in log-log scale) and regression slope, for $\alpha = 0.3$. $R^2 \approx 0.38$ is the coefficient of determination corresponding to the proportion of variance captured by the prediction with a slope of -0.3 (and adjusted averages).



(b) Slopes of the log-log regressions of $|\hat{u}_*^{(n)} - u_*|$ vs. n , for different values of α . $R^2 \approx 0.97$ is the coefficient of determination corresponding to the proportion of variance captured by the prediction of slopes given by exactly $-\alpha$.

Figure 4.3: Bias term: $|\hat{u}_*^{(n)} - u_*|$ and its decay rate for growing population size when $w_I^{(n)} \asymp n^{-\alpha}$, and comparison with the decay rate of $\log |\hat{u}_*^{(n)} - u_*|$ as $-\alpha \log(n)$.

Regression slopes for values of α larger than 0.5 have also been computed and their values suggest that this linear curve should be extended. This observation is still compatible with the conjectured order of variation of the bias and of the fluctuations due to the presence of multiplying factors, so that the values of n in the simulations are presumably too small to observe the predominance of the latter. For this reason, we restrict the right panel to $\alpha \leq 0.5$.

4.3 The very sparse case

We consider the very sparse case $\alpha = 0$ (and $a = 1$), where the number of edges in the graph is of the same order as the size of the population: $n w_E^{(n)} \asymp 1$, and thus $w_I^{(n)} \asymp 1$ (since $n \cdot w_E^{(n)} \cdot w_I^{(n)} = w = 3$). In particular Assumption 2.6 fails. By means of simulations, we observe that the integro-differential equation (2.11) is not a reliable description of the dynamics for n large in this case, thus highlighting the importance of Assumption 2.6.

More precisely, we consider constant $w_I^{(n)}$ (and hence constant $n w_E^{(n)} = w/w_I^{(n)}$), for values of $w_I^{(n)}$ that will be specified below but remain smaller than $w = 3$. Notice that this falls in the very sparse case, where Assumption 2.6 fails; the corresponding Erdős-Rényi graph is below the connectivity threshold and in the super-critical regime $n w_E^{(n)} \geq c > 1$, where there is a unique giant component containing a fraction of the population, and all other components have a size growing at most as $\log n$.

The intuition suggests that the infection dies out rapidly on all components other than the giant one (due to their small size), so that the effective population is rather given by the size of the giant component and not the size of the whole population. For this reason, we also study the proportion of infected individuals at time t in the giant component, which we will denote by $v^{(n)}(t)$ to avoid confusion with $u^{(n)}(t)$. To remove the fluctuations, we consider the temporal averages $\hat{u}_*^{(n)}$ as in (4.2) and $\hat{v}_*^{(n)}$ with analogous definition, replacing $u^{(n)}$ by $v^{(n)}$. We compare both $\hat{u}_*^{(n)}$ and $\hat{v}_*^{(n)}$ with u_* .

Our simulation results are shown in Fig. 4.4. Each point in Fig. 4.4 is derived from the average in

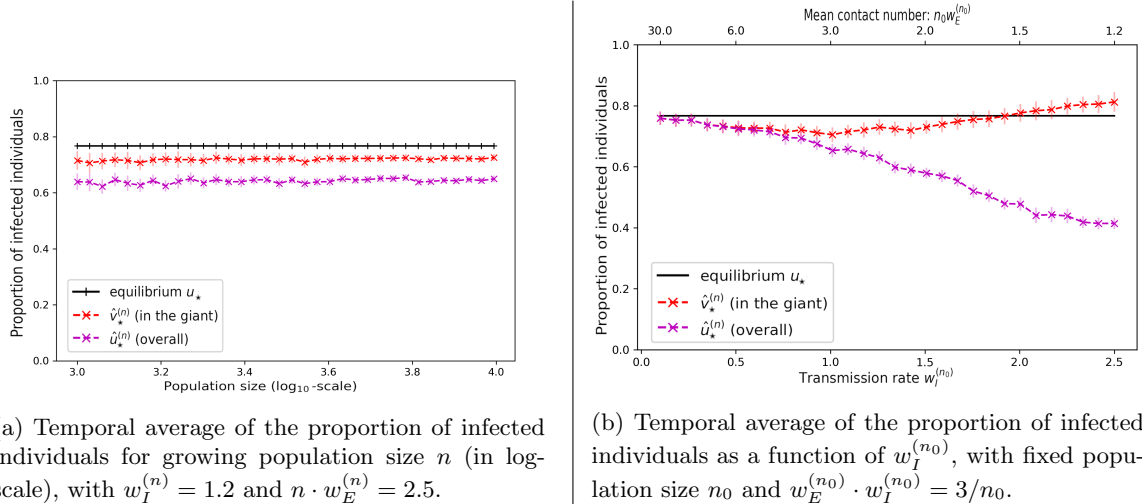


Figure 4.4: Very sparse yet super-critical regime: $n \cdot w_E^{(n)} = c$, with $c > 1$. Temporal averages $\hat{u}_*^{(n)}$ of the proportion of infected individuals w.r.t. the total population and $\hat{v}_*^{(n)}$ w.r.t. population of the giant component (each with whiskers for the ± 2 -standard-deviation intervals, with temporal standard deviation as in (4.2)), and comparison with the equilibrium u_* .

time, either $\hat{u}_*^{(n)}$ in purple or $\hat{v}_*^{(n)}$ in red, over a single run of epidemic. Intervals of fluctuations that account for twice the temporal standard deviations (either $2\hat{\sigma}_n$ or the analogous value estimated only over the individuals belonging to the giant component) are displayed with whiskers of the corresponding color. These intervals of fluctuations demonstrate that these temporal fluctuations play a negligible role in the trends.

In the left panel of Fig. 4.4, we present the temporal average of the proportion of infected individuals for the total population (that is, $\hat{u}_*^{(n)}$) and the population in the giant component (that is, $\hat{v}_*^{(n)}$), as a function of n , in the very sparse regime $\alpha = 0$ (with $w_I^{(n)} = 1.2$). Recall that $w = 3$, so that $n w_E^{(n)} = 2.5$ corresponds indeed to the supercritical regime, but the graph is not connected. We observe a convergence of the quantities $\hat{u}_*^{(n)}$ and $\hat{v}_*^{(n)}$ as n goes to infinity, but to a smaller value than the equilibrium u_* predicted by the model when the graph is dense or merely sparse. The restriction to the giant component entails a smaller discrepancy, implying that this effect is indeed contributing; however the discrepancy remains significant. This is all the more noticeable as the restriction to the giant component corresponds to a conditioning of the graph structure towards individuals having more contacts between each other.

In the right panel of Fig. 4.4, the size of the population is fixed to $n = n_0$, and we study the effect of $n w_E^{(n)}$ getting close to the transition phase $c = 1$, where the giant component disappears, by letting $w_I^{(n)}$ grow near 3. Similarly to the left panel, we plot the temporal average of the proportion of infected individuals for the total population (that is, $\hat{u}_*^{(n)}$) and the population in the giant component (that is, $\hat{v}_*^{(n)}$), but here as a function of $w_I^{(n)}$, for fixed $n = n_0$. When $w_I^{(n)}$ is close to 0, the coupling approximation is valid, that is, Assumption 2.6 holds, and almost all the population is in the giant component: thus we can apply our result and as expected the values of $\hat{u}_*^{(n)}$, $\hat{v}_*^{(n)}$ and u_* coincide. When we start increasing $w_I^{(n)}$, as already observed in the left panel, a discrepancy starts appearing between $\hat{u}_*^{(n)}$ and u_* , and between $\hat{v}_*^{(n)}$ and u_* , the latter being smaller. When increasing $w_I^{(n)}$ further, the effect of restricting the attention to the giant component becomes stronger: the discrepancy between $\hat{u}_*^{(n)}$ and u_* keeps increasing, while the one between $\hat{v}_*^{(n)}$ and u_*

remains small, and also changes sign when $w_I^{(n)}$ is larger than 2. The increase in the discrepancy when considering the whole population is largely due to a larger proportion of individuals outside of the giant component, among which the epidemic is not able to sustain itself.

5 Summary of contributions

Starting from a stochastic individual-based model of a finite population on a general state space of interactions, we established limit theorems showing that in large populations, the complex combination of randomness coming both from the graph structure and from the infection events can be treated as a small perturbation of a deterministic process. This deterministic process is described by an integro-differential equation, see (1.3) introduced in [DDZ22]. This integro-differential equation is ruled by a bounded recovery rate γ and a bounded transmission kernel w that combines these two aspects: the connection density and the infection rate.

Due to possible compensations between these two aspects, we do not rely on any form of convergence of the random graph sequence by itself. Instead, we propose an efficient coupling of the dynamics on a random graph structure (fixed in time) with a dynamics on a complete graph, in which there is no persistent graph structure and only the infections are random. By averaging over the proportion of individuals whose state can disagree between the two dynamics, we justify that their limits necessarily coincide as the size n of the population tends to infinity. The crucial condition for the coupling to provide a good approximation is that the average rate of infection over the population goes down to 0 as n tends to infinity (1.4).

We rely on very mild assumptions on the recovery rate function γ and the transmission kernel w . This allows to consider for w a wide variety of potential interactions networks (see Remark 2.1 and Assumption 2.3), such as discontinuous geometric kernels, continuous features on a multidimensional setting, and stochastic block models. Let us also stress that there is no assumption on the connectivity of the random graph $G^{(n)}$ of the population of size n : connectivity is not a relevant property for our convergence result.

Our convergence result holds in the case of dense and sparse graphs, where the total number of edges is, for a large population of size n , of order n/ϵ_n with $\lim_{n \rightarrow \infty} \epsilon_n = 0$, thus for example of order n^a with $a = 2$ (dense) and $a \in (1, 2)$ (sparse); see Remark 2.8. Assumption 2.6 fails in the case of very sparse graphs $a = 0$, for which the number of edges is of order $O(n)$ and thus the average rate of infection over the population is of order 1. It appears that Assumption 2.6 is crucial to ensure convergence as it is shown in simulations in Section 4.3.

Notice that the model could be easily generalized to allow the inclusion of non-Markovian description of the disease propagation, see [CTdA08, BR13, FPP21, FPPZN22, FRBC⁺22] in these directions. Also, there is no motion nor addition or deletion of individuals. For epidemics on moving particles, we can refer to [BEP22, DY22] for instance. Another important direction that could be included would be to relax the consideration of a static (in time) graph. When the epidemic spreads, the social network can be affected: either by preventive measure performed by separate individuals, who may drop edges and/or rewire connections depending on how the diseases progresses (e.g. [BB22]), or by public health measures such as lockdowns or contact-tracing (e.g. [CELT20, KS21]). This direction is also very important for future research.

Codes

All the codes and files necessary to reproduce the results presented in this document are available in the GitHub repository: https://forgemia.inra.fr/aurelien.velleret/simulations_containment_strategies_and_city_size_heterogeneity

Simulations and figures have been created in Python (v3.8.10) and many associated simulation outcomes are saved as csv files. Please refer to the Readme file for further information.

A Appendix: Proof of Proposition 3.6

We assume in this section that the hypotheses of Proposition 3.6 hold.

A.1 The epidemic process $\tilde{\eta}^{(n)}$ coupled to $\eta^{(n)}$

Recall the notations of Section 3. Following the classical graphical approach for defining interacting particle systems, see [Lig05, Section III.6] for reference, let us define a graphical model for the coupling as follows. Let $(V_\ell(i, j))_{1 \leq i < j, \ell \in \mathbb{N}^*}$ be a family of independent uniform random variables on $[0, 1]$, and independent of $\mathcal{X}^{(n)}$ and $\mathcal{E}^{(n)}$. We let $V_1(i, j)$ be equal to $V(i, j)$ from Section 3.1. Similarly to Section 3.1, we set $V_\ell(j, i) = V_\ell(i, j)$ and $V_\ell(i, i) = 0$ for convenience.

For each atom (s, i, j, u) of the Poisson measure Q_I , we draw an *arrow* from j to i at time s if $u \leq w_I^{(n)}(i, j)$, and denote the corresponding event by $\{u \leq w_I^{(n)}(i, j)\}$. Let us denote by $N_t^{(n)}(i, j)$ the number of arrows from j to i or vice-versa up to time t :

$$N_t^{(n)}(i_0, j_0) = \int \mathbb{1}_{\{s \leq t\}} \mathbb{1}_{\{\{i, j\} = \{i_0, j_0\}\}} \mathbb{1}_{\{u \leq w_I^{(n)}(i, j)\}} dQ_I. \quad (\text{A.1})$$

For any atom of Q_I that leads to an arrow, we define the connection events:

$$C^{(n)}(i, j, u, s) = \{u \leq w_I^{(n)}(i, j)\} \cap \{V_1(i, j) \leq w_E^{(n)}(i, j)\} = \{u \leq w_I^{(n)}(i, j)\} \cap \{i \sim j\}, \quad (\text{A.2})$$

$$\tilde{C}^{(n)}(i, j, u, s) = \{u \leq w_I^{(n)}(i, j)\} \cap \{V_{N_s^{(n)}(i, j)}(i, j) \leq w_E^{(n)}(i, j)\}. \quad (\text{A.3})$$

On C (resp. \tilde{C}), we say that the arrow is activated for the original process (resp. for the coupled process). As usual for graphical models, $\eta^{(n)}$ (resp. $\tilde{\eta}^{(n)} = (\tilde{\eta}_t^{(n)})_{t \in \mathbb{R}_+}$) is then constructed by following the activated arrows defined by $C^{(n)}$ (resp. $\tilde{C}^{(n)}$). Compared to (3.2), the dynamics of $\tilde{\eta}^{(n)}$ is the same as the one of $\eta^{(n)}$ except that the event $\{i \sim j\} \cap \{u \leq w_I^{(n)}(x_i, x_j)\}$ is replaced by the connection event $\tilde{C}^{(n)}(i, j, u, s)$. If the arrow is the first to occur between i and j , then $N_s^{(n)}(i, j) = 1$ and the events are the same, if not, the use of an independent $V_\ell(i, j)$ in the definition of $\tilde{C}^{(n)}$ corresponds to a resampling of the connection between i and j .

Thus, the epidemic process $\tilde{\eta}^{(n)} = (\tilde{\eta}_t^{(n)})_{t \in \mathbb{R}_+} \in \mathcal{D}$ on the n individuals $\mathcal{X}^{(n)} = (x_i)_{i \in [1, n]}$ is defined by:

$$\tilde{\eta}_t^{(n)}(dx, de) = \frac{1}{n} \sum_{i=1}^n \delta_{(x_i, \tilde{E}_t^i)}(dx, de), \quad (\text{A.4})$$

with $\tilde{\eta}_0^{(n)} = \eta_0^{(n)}$ and, similarly to (3.4), for $t > 0$:

$$\begin{aligned} \tilde{\eta}_t^{(n)} - \tilde{\eta}_0^{(n)} &= n^{-1} \int \mathbb{1}_{\{s < t\}} (\delta_{(x_i, S)} - \delta_{(x_i, I)}) \mathbb{1}_{\tilde{A}^{(n)}(i, u, s)} dQ_R \\ &\quad + n^{-1} \int \mathbb{1}_{\{s < t\}} (\delta_{(x_i, I)} - \delta_{(x_i, S)}) \mathbb{1}_{\tilde{B}^{(n)}(i, j, u, s)} dQ_I, \end{aligned} \quad (\text{A.5})$$

where $\tilde{A}^{(n)}(i, u, s)$ and $\tilde{B}^{(n)}(i, j, u, s)$ are defined similarly to (3.1) and (3.2):

$$\tilde{A}^{(n)}(i, u, s) = \{i \leq n\} \cap \{u \leq \gamma^{(n)}(x_i)\} \cap \{\tilde{E}_{s-}^i = I\},$$

and

$$\tilde{B}^{(n)}(i, j, u, s) = \{i, j \leq n\} \cap \tilde{C}^{(n)}(i, j, u, s) \cap \{\tilde{E}_{s-}^i = S, \tilde{E}_{s-}^j = I\}.$$

From this description, we get that $\tilde{\eta}^{(n)}$ is an epidemic process on a complete graph (so the corresponding connection density is $\tilde{w}_E^{(n)} \equiv 1$) with the infection rate $\tilde{w}_I^{(n)} = w_I^{(n)} w_E^{(n)} = n^{-1} w^{(n)}$ and recovery rate $\tilde{\gamma}^{(n)} = \gamma^{(n)}$.

A.2 The fog process

To study the coupling between $\eta^{(n)}$ and $\tilde{\eta}^{(n)}$, we introduce a process that we call the *fog* process, that we first describe informally. At time t , each vertex i is either in or out of the fog: $\xi_t^{(n)}(i) = 1$ or 0. At the beginning there is no fog ($\xi_0^{(n)}(i) = 0$). Once a vertex enters the fog it stays foggy forever. The rules for creating the fog or propagating it will ensure the following key property:

If $\xi_t^{(n)}(i) = 0$, then the processes $\eta^{(n)}$ and $\tilde{\eta}^{(n)}$ coincide at vertex i on the time interval $[0, t]$.

In other words, the fog is an upper bound on the vertices where the processes $\eta^{(n)}$ and $\tilde{\eta}^{(n)}$ may have decoupled. The fog process is formally a family of pure-jump processes $\xi^{(n)}(i) = (\xi_t^{(n)}(i))_{t \in \mathbb{R}_+}$, that start at 0 and jump at most once, to the value 1. Consider the following conditions:

- a) The vertex i is not currently in the fog: $\xi_{t-}^{(n)}(i) = 0$.
- b) There is an arrow at time t from some j to i .
- c) The vertex j is in the fog, and the arrow is activated for the coupled process.
- c') The arrow is activated for exactly one of the two processes.

If a), b) and c) are satisfied, we say that the fog *propagates* from j to i , and that i is the *child* of j ; otherwise, if a), b) and c') hold, we say that i is a *root* for the fog process. In both cases i enters the fog at time t : $\xi_t^{(n)}(i) = 1$. Formally the propagation of the fog, that is conditions a), b) and c), corresponds to the event:

$$H_{\text{prop}}^{(n)}(i, j, u, s) = \{i, j \leq n\} \cap \{\xi_{s-}^{(n)}(i) = 0\} \cap \tilde{C}^{(n)}(i, j, u, s) \cap \{\xi_{s-}^{(n)}(j) = 1\}, \quad (\text{A.6})$$

and the conditions a), b) and c') to the event:

$$H_{\text{xor}}^{(n)}(i, j, u, s) = \{i, j \leq n\} \cap \{\xi_{s-}^{(n)}(i) = 0\} \cap \left(C^{(n)}(i, j, u, s) \Delta \tilde{C}^{(n)}(i, j, u, s) \right),$$

where $A \Delta B = (A \cap B^c) \cup (A^c \cap B)$. In particular becoming a root corresponds to the event:

$$H_{\text{root}}^{(n)}(i, j, u, s) = H_{\text{prop}}^{(n)}(i, j, u, s)^c \cap H_{\text{xor}}^{(n)}(i, j, u, s). \quad (\text{A.7})$$

In particular, notice that if at time s , j is in the fog, the arrow from j to i is activated and i is not previously in the fog (that is we are on the event $C^{(n)}(i, j, u, s) \cup \tilde{C}^{(n)}(i, j, u, s)$), then i is now in the fog (this corresponds to the events a), b) and c) or c')).

We can formalize the evolution of $\xi^{(n)}$ as follow, for $i \in \llbracket 1, n \rrbracket$:

$$\xi_t^{(n)}(i') = \int \mathbb{1}_{\{s \leq t\}} \mathbb{1}_{H^{(n)}(i, j, u, s)} \mathbb{1}_{\{i=i'\}} dQ_I^{(n)}, \quad (\text{A.8})$$

where $H^{(n)}(i, j, u, s)$ specifies that i enters the fog at time s :

$$H^{(n)}(i, j, u, s) = H_{\text{prop}}^{(n)}(i, j, u, s) \cup H_{\text{root}}^{(n)}(i, j, u, s).$$

Let us denote the number of vertices in the fog at time t by:

$$\Xi_t^{(n)} = \sum_{i \in \llbracket 1, n \rrbracket} \xi_t^{(n)}(i). \quad (\text{A.9})$$

The fog process is designed to ensure the following upper bound.

Lemma A.1 (Control of the coupling by the fog process). *The following upper-bound holds a.s. for all $T \geq 0$:*

$$\sup_{\{t \leq T\}} \|\eta_t^{(n)} - \tilde{\eta}_t^{(n)}\|_{TV} \leq \frac{1}{n} \Xi_T^{(n)}.$$

Proof. Since by definition $\eta_0^{(n)} = \tilde{\eta}_0^{(n)}$ and $\xi_0^{(n)} = 0$ and that the same individuals in the two epidemic processes when infected recover at the same time (the recovery procedure is driven by the same Poisson point measure Q_R), we get by construction that the number of points in the support of $\xi_t^{(n)}$ is then, after careful consideration, an upper bound of the number of vertices with different states in $\eta_t^{(n)}$ and $\tilde{\eta}_t^{(n)}$. More precisely, the following upper-bound holds a.s. for all $t \geq 0$ and all $i \in \llbracket 1, n \rrbracket$:

$$\mathbb{1}_{\{E_t^i \neq \tilde{E}_t^i\}} \leq \xi_t^{(n)}(i) \in \{0, 1\}.$$

Using that the process $(\xi_t^{(n)}(i))_{t \in \mathbb{R}_+}$ is non-decreasing, and the expressions (2.2) for $\eta_t^{(n)}$ and (A.4) for $\tilde{\eta}_t^{(n)}$, we deduce that:

$$\sup_{t \in [0, T]} \|\eta_t^{(n)} - \tilde{\eta}_t^{(n)}\|_{TV} \leq \frac{1}{n} \sup_{\{t \leq T\}} \Xi_t^{(n)} = \frac{1}{n} \Xi_T^{(n)}.$$

□

A.3 Upper bound on the expected size of the fog

We follow ideas from [PB19, Section 1.2] where “ghost infections” are introduced to associate the SIR infection process with a branching infection process (the first being included in the second for the chosen coupling). Using the construction of $(\xi_t^{(n)})_{t \in \mathbb{R}_+}$, we can represent its support in terms of random forests. More precisely, recall that each time a vertex enters the fog, it is either as a *root* or as a *child* of another vertex that is already in the fog at that time.

We denote by S_i the jumping time of $\xi^{(n)}(i)$ (with the convention that $S_i = +\infty$ if $\xi_\infty^{(n)}(i) = 0$), by $\mathcal{R}^{(n)}$ the set of roots and by $\mathcal{R}_t^{(n)} \subset \llbracket 1, n \rrbracket$ the set of roots born up to time t :

$$\mathcal{R}_t^{(n)} = \{i \in \mathcal{R}^{(n)} : S_i \leq t\}. \quad (\text{A.10})$$

For a given root i , let $\xi^{i, (n)}$ denote the process of its descendants, for $t \geq 0$ and $i' \in \llbracket 1, n \rrbracket$:

$$\xi_t^{i, (n)}(i') = \mathbb{1}_{\{i \text{ is a root}\}} \mathbb{1}_{\{i' \text{ is a descendant of } i\}} \xi_t^{(n)}(i').$$

Let $\Xi_t^{i, (n)} = \sum_{i' \in \llbracket 1, n \rrbracket} \xi_t^{i, (n)}(i')$ be the total population up to time t fathered by the root i , and notice that $\Xi_t^{i, (n)} = 0$ on $\{t < S_i\}$. The total size of the fog is therefore:

$$\Xi_t^{(n)} = \sum_{i=1}^n \Xi_t^{i, (n)} \mathbb{1}_{\{i \in \mathcal{R}_t^{(n)}\}}. \quad (\text{A.11})$$

We now give an upper bound on $\mathbb{E} \left[\Xi_t^{i, (n)} \mathbb{1}_{\{i \in \mathcal{R}_t^{(n)}\}} \right]$. Recall $C_w = \sup_{n \in \mathbb{N}^*} \|w^{(n)}\|_\infty$.

Lemma A.2. *The following upper-bound holds for all $t \geq 0$ and $i \in \llbracket 1, n \rrbracket$:*

$$\mathbb{E} \left[\Xi_t^{i, (n)} \mathbb{1}_{\{i \in \mathcal{R}_t^{(n)}\}} \right] \leq e^{C_w t} \mathbb{P} \left(i \in \mathcal{R}_t^{(n)} \right).$$

Proof. To avoid any confusion with the notation $dQ_I = Q_I(ds, di, dj, du)$, we shall prove the lemma with i replaced by i_0 . By construction (recalling (A.8), (A.14), (A.11) and (A.12)), the evolution of $\xi^{i_0, (n)}$ is given by the following formula, for $i' \in \llbracket 1, n \rrbracket$:

$$\xi_t^{i_0, (n)}(i') = \mathbb{1}_{\{i_0 \in \mathcal{R}_t^{(n)}\}} \mathbb{1}_{\{i' = i_0\}} + \mathbb{1}_{\{t \geq S_{i_0}\}} \int \mathbb{1}_{\{s \leq t\}} \mathbb{1}_{D^{i_0, (n)}(i, j, u, s)} \mathbb{1}_{\{i' = i\}} dQ_I^{(n)}, \quad (\text{A.12})$$

where $D^{i_0, (n)}(i, j, u, s)$ specifies that, at time s , i enters the fog as a child of a vertex j which, itself, descends from i_0 (compare with $H_{\text{prop}}^{(n)}$ from (A.6)):

$$D^{i_0, (n)}(i, j, u, s) = \{i, j \leq n\} \cap \{\xi_{s-}^{i_0, (n)}(i) = 0\} \cap \{\xi_{s-}^{i_0, (n)}(j) = 1\} \cap \tilde{C}^{(n)}(i, j, u, s).$$

On the event $\{i_0 \in \mathcal{R}^{(n)}\}$, since $n \cdot w_E^{(n)}(x, y) \cdot w_I^{(n)}(x, y) \leq C_w$ holds for any $x, y \in \mathbb{X}$, the process $(\xi_{S_{i_0}+t}^{i_0, (n)})_{t \in \mathbb{R}_+}$ jumps with an additional Dirac Mass at location i' with a rate upper-bounded at time t by

$$\sum_{j \in \llbracket 1, n \rrbracket} \mathbb{1}_{\{\xi_{S_{i_0}+t-}^{i_0, (n)}(j) \geq 1\}} w_E^{(n)}(x_{i'}, x_j) \cdot w_I^{(n)}(x_{i'}, x_j) \leq \frac{C_w}{n} \sum_{j \in \llbracket 1, n \rrbracket} \mathbb{1}_{\{\xi_{S_{i_0}+t-}^{i_0, (n)}(j) \geq 1\}}.$$

Thus, this process is stochastically dominated by the pure-jump process $\zeta^{(n)} = (\zeta_t^{(n)})_{t \in \mathbb{R}_+}$ on $\llbracket 1, n \rrbracket$ defined by:

$$\zeta_t^{(n)}(i') = \mathbb{1}_{\{i' = i_0\}} + \int \mathbb{1}_{\{s \leq t\}} \mathbb{1}_{G^{(n)}(i, j, k, z, s)} \mathbb{1}_{\{i' = i\}} Q(ds, di, dj, dk, dz),$$

where Q is a Poisson point measure on $\mathbb{R}_+ \times \mathbb{N}^* \times \mathbb{N}^* \times \mathbb{N}^* \times \mathbb{R}_+$ with intensity $ds n(di) n(dj) n(dk) dz$ and $G^{(n)}(i, j, k, z, s)$ specifies that, at time s , an individual is added at vertex i as a descendant of an already added individual at vertex j (the parameter k being introduced to cope with the allowed multiplicity of individuals at position j):

$$G^{(n)}(i, j, k, z, s) = \{i, j \leq n\} \cap \{k \leq \zeta_{s-}^{(n)}(j)\} \cap \{z \leq C_w/n\}.$$

Let $Z^{(n)} = (Z_t^{(n)})_{t \in \mathbb{R}_+}$ be the size of the population at time t defined by $Z_t^{(n)} = \sum_{i \in \llbracket 1, n \rrbracket} \zeta_t^{(n)}(i)$. $Z^{(n)}$ is expressed as follows for any $t \geq 0$:

$$Z_t^{(n)} = 1 + \int \mathbb{1}_{\{s \leq t\}} \mathbb{1}_{G^{(n)}(i, j, k, z, s)} dQ = 1 + \frac{C_w}{n} \int \mathbb{1}_{\{s \leq t\}} n Z_s^{(n)} ds + W_t^{(n)},$$

where $W^{(n)} = (W_t^{(n)})_{t \in \mathbb{R}_+}$ is a square integrable martingale with quadratic variation:

$$\langle W^{(n)} \rangle_t = \frac{C_w}{n} \int_0^t n Z_s^{(n)} ds = C_w \int_0^t Z_s^{(n)} ds.$$

We recognize the semi-martingale decomposition of a birth process with birth rate C_w , started at 1. Thus, we have $\mathbb{E}[Z_t^{(n)}] = \exp(C_w t)$.

We deduce that on the event $\{i_0 \in \mathcal{R}^{(n)}\}$, the total mass $\Xi_{S_{i_0}+t}^{i_0, (n)}$ is stochastically dominated by $Z_t^{(n)}$. Since the process $\Xi^{i_0, (n)}$ is non-decreasing and 0 on $\{S_{i_0} > t\}$, we deduce that:

$$\mathbb{E} \left[\Xi_t^{i_0, (n)} \mathbb{1}_{\{i_0 \in \mathcal{R}_t^{(n)}\}} \right] \leq \mathbb{E} \left[\Xi_{S_{i_0}+t}^{i_0, (n)} \mathbb{1}_{\{i_0 \in \mathcal{R}_t^{(n)}\}} \right] \leq \mathbb{P} \left(i_0 \in \mathcal{R}_t^{(n)} \right) \mathbb{E}[Z_t^{(n)}].$$

This concludes the proof. \square

The following lemma gives a bound on the probability for a given vertex to be a root before a given time t .

Lemma A.3. *The following upper-bound holds for all $t \geq 0$ and all $i \in \llbracket 1, n \rrbracket$:*

$$\mathbb{P}\left(i \in \mathcal{R}_t^{(n)} \mid \mathcal{X}^{(n)}\right) \leq \frac{2t(t \vee 1)C_w}{n} \sum_{j \in \llbracket 1, n \rrbracket, j \neq i} \left\{ (w_I^{(n)}(x_i, x_j) \wedge 1) + (w_I^{(n)}(x_j, x_i) \wedge 1) \right\}.$$

Proof. Let $t > 0$, $n \geq 2$ and $i \in \llbracket 1, n \rrbracket$ be fixed. By construction, the number of activations $(N_t^{(n)}(i, j))_{j \in \mathbb{N}^*, i \neq j}$ are independent Poisson random variable with respective parameter $t W_I^{(n)}(x_i, x_j)$ where:

$$W_I^{(n)}(x, y) = w_I^{(n)}(x, y) + w_I^{(n)}(y, x). \quad (\text{A.13})$$

If $i \in \mathcal{R}^{(n)}$ is a root born at (finite) time S_i , we denote by (S_i, i, J_i, U_i) the unique atom of the random measure Q_I at time S_i , and let $C_i = C(i, J_i, U_i, S_i)$ (resp. $\tilde{C}_i = \tilde{C}(i, J_i, U_i, S_i)$) be the event that the arrow that leads to the creation of the root i is activated for the original process (resp. for the coupled process). By the definition of roots, see (A.7), the following inclusion holds for all $i \in \llbracket 1, n \rrbracket$ and all $t \in \mathbb{R}_+$:

$$\{i \in \mathcal{R}_t^{(n)}\} \subset \{S_i \leq t\} \cap (C_i \Delta \tilde{C}_i). \quad (\text{A.14})$$

By construction, see (A.2) and (A.3), on the symmetric difference $C_i \Delta \tilde{C}_i$, the number of arrows between $\{i, j\}$ up to time S_i , that is $L_i := N_{S_i}^{(n)}(i, J_i)$ must be larger than 2. Thus, the following sequence of inclusions holds:

$$\begin{aligned} \{i \in \mathcal{R}_t^{(n)}\} &\subset \{S_i \leq t\} \cap \{L_i \geq 2\} \cap (C_i \cup \tilde{C}_i) \\ &\subset \{S_i \leq t\} \cap \{L_i \geq 2\} \cap \left(\{V_{L_i}(i, J_i) \leq w_E^{(n)}(x_i, x_{J_i})\} \cup \{V_1(i, J_i) \leq w_E^{(n)}(x_i, x_{J_i})\} \right) \\ &\subset \{N_t^{(n)}(i, J_i) \geq 2\} \cap \{\exists \ell \in \llbracket 1, N_t^{(n)}(i, J_i) \rrbracket \text{ such that } V_\ell(i, J_i) \leq w_E^{(n)}(x_i, x_{J_i})\}. \end{aligned}$$

By construction, for $j \neq i$, the random variables $N_t^{(n)}(i, j)$ and $V_\ell(i, j)$ for $\ell \in \mathbb{N}^*$ are independent and the latter are uniformly distributed on $[0, 1]$. We deduce that:

$$\begin{aligned} &\mathbb{P}\left(i \in \mathcal{R}_t^{(n)} \mid \mathcal{X}^{(n)}\right) \\ &\leq \sum_{j \in \llbracket 1, n \rrbracket, j \neq i} \mathbb{P}\left(N_t^{(n)}(i, j) \geq 2, \exists \ell \in \llbracket 1, N_t^{(n)}(i, j) \rrbracket \text{ such that } V_\ell(i, j) \leq w_E^{(n)}(x_i, x_j) \mid \mathcal{X}^{(n)}\right) \\ &= \sum_{j \in \llbracket 1, n \rrbracket, j \neq i} g\left(t W_I^{(n)}(x_i, x_j), w_E^{(n)}(x_i, x_j)\right), \end{aligned}$$

with:

$$g(\theta, r) = \mathbb{P}_\theta\left(L \geq 2, \exists \ell \in \llbracket 1, L \rrbracket \text{ such that } V_\ell \leq r\right),$$

where under \mathbb{P}_θ , L is distributed as a Poisson random variable with parameter θ and $(V_\ell)_{\ell \in \mathbb{N}^*}$ as independent random variables uniformly distributed on $[0, 1]$ and independent of L . Elementary computations give:

$$\begin{aligned} g(\theta, r) = \mathbb{P}_\theta\left(L \geq 2, \exists \ell \in \llbracket 1, L \rrbracket \text{ such that } V_\ell \leq r\right) &= \sum_{k=2}^{\infty} \frac{\theta^k}{k!} e^{-\theta} \left(1 - (1-r)^k\right) \\ &= 1 - e^{-\theta r} - \theta r e^{-\theta} \\ &\leq \theta r (\theta \wedge 1), \end{aligned}$$

where for the inequality, we used that $1 - e^{-x}$ is less than x and $x \wedge 1$. Since $w^{(n)} = n w_I^{(n)} w_E^{(n)}$ is bounded by C_w , we get that $t W_I^{(n)} w_E^{(n)} \leq 2t C_w/n$ (recall also the link between $W_I^{(n)}$ and $w_I^{(n)}$ in (A.13) and the symmetry of $w_E^{(n)}$). We obtain that:

$$\mathbb{P}\left(i \in \mathcal{R}^{(n)} \mid \mathcal{X}^{(n)}\right) \leq \frac{2t C_w}{n} \sum_{j \in \llbracket 1, n \rrbracket, j \neq i} \left((t w_I^{(n)}(x_i, x_j)) \wedge 1 \right) + \left((t w_I^{(n)}(x_j, x_i)) \wedge 1 \right).$$

This concludes the proof. \square

A.4 Conclusion

Using Lemma A.1, Equation (A.11), Lemmas A.2 and A.3, as well as the definition of \mathcal{I}_n in (2.9), we deduce that:

$$\mathbb{E}\left[\sup_{\{t \leq T\}} \|\eta_t^{(n)} - \tilde{\eta}_t^{(n)}\|_{TV}\right] \leq \frac{1}{n} \mathbb{E}\left[\Xi_T^{(n)}\right] = \frac{1}{n} \sum_{i=1}^n \mathbb{E}\left[\Xi_T^{i,(n)}\right] \leq C_T \mathcal{I}_n(w_I^{(n)} \wedge 1),$$

with $C_T = 4T(T \vee 1) C_w e^{C_w T}$. This concludes the proof of Proposition 3.6.

Acknowledgements

The author would like to thank the anonymous referee for their diligent and professional work.

References

- [AB00] H. Andersson and T. Britton. *Stochastic Epidemic Models and Their Statistical Analysis*. Springer New York, 2000.
- [Abb18] E. Abbe. Community detection and Stochastic Block Models: recent development. *J. Machine Learning Res.*, 18(177):1–86, 2018.
- [AN22] G. Aletti and G. Naldi. Opinion dynamics on graphon: the piecewise constant case. *Appl. Math. Lett.*, 133:108227, 2022.
- [And98] H. Andersson. Limit theorems for a random graph epidemic model. *Ann. Appl. Probab.*, 8(4):1331–1349, 1998.
- [And99] H. Andersson. Epidemic models and social networks. *Math. Scientist*, 24(2):128–147, 1999.
- [APSS20] M. Avella-Medina, F. Parise, M. T. Schaub, and S. Segarra. Centrality measures for graphons: Accounting for uncertainty in networks. *IEEE Transactions on Network Science and Engineering*, 7(1):520–537, 2020.
- [ARGL22] A. Aurell, C. René, D. Gökçe, and M. Laurière. Finite state graphon games with applications to epidemics. *Dyn. Games Appl.*, 12(1):49–81, 2022.
- [BB22] F. Ball and T. Britton. Epidemics on networks with preventive rewiring. *Random Structures & Algorithms*, 61(2):250–297, 2022.
- [BCL⁺11] C. Borgs, J. Chayes, L. Lovász, V. Sós, and K. Vesztegombi. Limits of randomly grown graph sequences. *European J. Comb.*, 32(7):985–999, 2011.

- [BEP22] S. Bowong, A. Emakoua, and E. Pardoux. A spatial stochastic epidemic model: law of large numbers and central limit theorem. *Stoch. PDE: Anal. Comp.*, 2022.
- [Bil99] P. Billingsley. *Convergence of Probability Measures*. Wiley Series in Probability and Statistics. John Wiley & Sons, Inc., New York, second edition edition, 1999.
- [BLRT22] S. Billiard, H. Leman, T. Rey, and V.C. Tran. Continuous limits of large plant-pollinator random networks and some applications. arxiv:2201.05219, 2022.
- [BN08] F. Ball and P. Neal. Network epidemic models with two levels of mixing. *Math. Biosci.*, 212:69–87, 2008.
- [Bol79] B. Bollobás. *Graph theory*, volume 63. Springer, New York, 1979.
- [Bor16] C. Bordenave. *Lecture notes on random graphs and probabilistic combinatorial optimization*. <https://www.math.univ-toulouse.fr/~bordenave/coursRG.pdf>, 2016.
- [BR13] A.D. Barbour and G. Reinert. Approximating the epidemic curve. *Electron. J. Probab.*, 18(54):2557, 2013.
- [BS01] I. Benjamini and O. Schramm. Recurrence of distributional limits of finite planar graphs. *Electron. J. Probab.*, 6:1–13, 2001.
- [CELT20] A. Charpentier, R. Elie, M. Laurière, and V.C. Tran. Covid-19 pandemic control: balancing detection policy and lockdown intervention under ICU sustainability. *Math. Model. Nat. Phenom.*, 15:57, 2020.
- [CTdA08] S. Cléménçon, V.C. Tran, and H. de Arazoza. A stochastic SIR model with contact-tracing: large population limits and statistical inference. *J. Biol. Dyn.*, 2(4):391–414, 2008.
- [DDMT12] L. Decreusefond, J.-S. Dhersin, P. Moyal, and V.C. Tran. Large graph limit for a SIR process in random network with heterogeneous connectivity. *Ann. Appl. Probab.*, 22(2):541–575, 2012.
- [DDZ22] J.-F. Delmas, D. Dronnier, and P.-A. Zitt. An infinite-dimensional metapopulation SIS model. *J. Differ. Equ.*, 313:1–53, 2022.
- [DDZ23] J.-F. Delmas, D. Dronnier, and P.-A. Zitt. Optimal vaccination: Various (counter) intuitive examples. *J. Math. Bio.*, 86:1–57, 2023.
- [Dur07] R. Durrett. *Random graph dynamics*. Cambridge University Press, New York, 2007.
- [DY22] R. Durrett and D. Yao. Susceptible–infected epidemics on evolving graphs. *Electronic Journal of Probability*, 27:1 – 66, 2022.
- [FM04] N. Fournier and S. Méléard. A microscopic probabilistic description of a locally regulated population and macroscopic approximations. *Ann. Appl. Probab.*, 14(4):1880–1919, 2004.
- [FPP21] R. Forien, G. Pang, and E. Pardoux. Epidemic models with varying infectivity. *SIAM J. Appl. Math.*, 81(5):1893–1930, 2021.
- [FPPZN22] R. Forien, G. Pang, E. Pardoux, and A.B. Zotsa-Ngoufack. Stochastic epidemic models with varying infectivity and susceptibility. arXiv:2210.04667, 2022.

- [FRBC⁺22] F. Foutel-Rodier, F. Blanquart, P. Courau, P. Czuppon, J.-J. Duchamps, J. Gamblin, E. Kerdoncuff, R. Kulathinal, L. Régnier, L. Vuduc, A. Lambert, and E. Schertzer. From individual-based epidemic model to McKendrick-von Foerster PDEs: a guide to modeling and inferring COVID-19 dynamics. *J. Math. Biol.*, 85(43), 2022.
- [GKS20] N. Georgiou, I.Z. Kiss, and P.L. Simon. Theoretical and numerical considerations of the assumptions behind triple closures in epidemic models on networks. In R.P. Mondaini, editor, *Trends in biomathematics: modeling cells, flows, epidemics, and the environment*, pages 209–234, Switzerland AG, 2020. Springer.
- [Hou12] T. House. Modelling epidemics on networks. *Contemp. Phys.*, 53(3):213–225, 2012.
- [IW89] N. Ikeda and S. Watanabe. *Stochastic Differential Equations and Diffusion Processes*, volume 24. North-Holland Publishing Company, 1989. Second Edition.
- [JLW14] S. Janson, M. Luczak, and P. Windridge. Law of large numbers for the SIR epidemic on a random graph with given degrees. *Random Structures & Algorithms*, 45(4):726–763, 2014.
- [JS87] J. Jacod and A.N. Shiryaev. *Limit Theorems for Stochastic Processes*. Springer-Verlag, Berlin, 1987.
- [KHT22] D. Keliger, I. Horváth, and B. Takács. Local-density dependent Markov processes on graphons with epidemiological applications. *Stoch. Proc. Appl.*, 148:324–352, 2022.
- [KM32] W.O. Kermack and A.G. McKendrick. Contributions to the Mathematical Theory of Epidemics. II. The Problem of Endemicity. *Proc. Roy. Soc. Lond. A*, 138(834):55–83, 1932.
- [KM33] W.O. Kermack and A.G. McKendrick. Contributions to the mathematical theory of epidemics. iii.—further studies of the problem of endemicity. *Proc. R. Soc. Lond. A*, 141:94–122, 1933.
- [KMS17] I.Z. Kiss, J.C. Miller, and P. Simon. *Mathematics of Epidemics on Networks*, volume 46 of *Interdisciplinary Applied Mathematics*. Springer, 1 edition, 2017.
- [KS21] I. Kryven and C. Stegehuis. Contact tracing in configuration models. *Journal of Physics: Complexity*, 2(2):025004, 2021.
- [KT19] C. Kuehn and S. Throm. Power network dynamics on graphons. *SIAM J. Appl. Math.*, 79(4):1271–1292, 2019.
- [Lig05] T. M. Liggett. *Interacting particle systems*. Classics in Mathematics. Springer-Verlag, Berlin, 2005. Reprint of the 1985 original.
- [Lov12] L. Lovász. *Large networks and graph limits*, volume 60 of *Colloquium publications*. American Mathematical Society, 2012.
- [Mil11] J.C. Miller. A note on a paper by Erik Volz: SIR dynamics in random networks. *J. Math. Biol.*, 62(3):349–358, 2011.
- [New02] M.E.J. Newman. The spread of epidemic disease on networks. *Physical Reviews E*, 66, 2002.
- [New03] M.E.J. Newman. The structure and function of complex networks. *SIAM Review*, 45:167–256, 2003.

- [NP22] G. Naldi and G. Patanè. A graph-based modelling of epidemics: Properties, simulation, and continuum limit. *arXiv:2208.07559*, 2022.
- [PB19] E. Pardoux and T. Britton. *Stochastic Epidemic Models with Inference*. Lecture Notes in Mathematics 2255. Springer, 2019.
- [Pen03] M. Penrose. *Random geometric graphs*, volume 5 of *Oxford Studies in Probability*. Oxford University Press, Oxford, 2003.
- [Per99] E. A. Perkins. Dawson-Watanabe superprocesses and measure-valued diffusions. In *Ecole d'Été de Probabilités de Saint-Flour*, volume 1781 of *Lecture Notes in Math.*, pages 125–329, New York, 1999.
- [vdH17] R. van der Hofstad. *Random Graphs and Complex Networks*, volume 1 of *Cambridge Series Stat. Probab. Math.* Cambridge University Press, Cambridge, 2017.
- [vdH24] R. van der Hofstad. *Random Graphs and Complex Networks*. Cambridge Series in Statistical and Probabilistic Mathematics. Cambridge University Press, 2024.
- [vdHJvL10] R. van der Hofstad, A.J.E.M. Janssen, and J.S.H. van Leeuwaarden. Critical epidemics, random graphs, and Brownian motion with a parabolic drift. *Adv. Appl. Prob.*, 42:1187–1206, 2010.
- [VFG20] R. Vizuete, P. Frasca, and F. Garin. Graphon-based sensitivity analysis of SIS epidemics. *IEEE Control Systems Letters*, 4(3):542–547, 2020.
- [Vol08] E. Volz. SIR dynamics in random networks with heterogeneous connectivity. *Math. Biol.*, 56:293–310, 2008.